Prognostic Association of Immunoproteasome Expression and its Correlation with Tumor-Infiltrating Lymphocytes in Breast Cancer

A Thesis

submitted to

Indian Institute of Science Education and Research Pune in partial fulfilment of the requirements for the BS-MS Dual Degree Programme

by

Sampada Deepak Ghute

Indian Institute of Science Education and Research Pune

Dr. Homi Bhabha Road,

Pashan, Pune 411008, INDIA.

Date: 28 March, 2025

Under the guidance of

Supervisor: Dr. Madhura Kulkarni,

Centre for Translational Cancer Research: A Joint Initiative of Indian Institute of Science Education and Research (IISER), Pune and Prashanti Cancer Care Mission (PCCM), Pune

From May 2024 to Mar 2025

INDIAN INSTITUTE OF SCIENCE EDUCATION AND RESEARCH PUNE

Certificate

This is to certify that this dissertation entitled Prognostic Association of Immunoproteasome Expression and its Correlation with Tumor-Infiltrating Lymphocytes in Breast Cancer towards the partial fulfilment of the BS-MS dual degree programme at the Indian Institute of Science Education and Research, Pune represents study/work carried out by Sampada Ghute at Indian Institute of Science Education and Research under the supervision of Dr. Madhura Kulkarni, CTCR, PCCM, Pune during the academic year 2024-2025.

Dr. Madhura Kulkarni

Committee:

Dr. Madhura Kulkarni

Prof. Satyajit Rath

I dedicate this thesis to Dr. Madhura Kulkarni, whose guidance, support, and passion for research have been truly inspiring. I could not have made it through this journey without her guidance, kindness, and relentless encouragement.

Declaration

I hereby declare that the matter embodied in the report entitled “Prognostic Association of Immunoproteasome Expression and its Correlation with Tumor-Infiltrating Lymphocytes in Breast Cancer” are the results of the work carried out by me at the Department of Biology, Indian Institute of Science Education & Research (IISER) Pune, under the supervision of Dr. Madhura Kulkarni, and the same has not been submitted elsewhere for any other degree. Wherever others contribute, every effort is made to indicate this clearly, with due reference to the literature and acknowledgement of collaborative research and discussions.

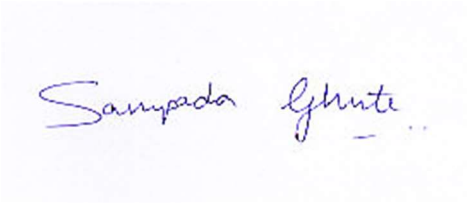

Sampada Ghute

20201217

Contents

List of Tables 7

List of Figures 7

Abstract 9

Acknowledgments 10

Contributions 11

1. Introduction 12

    1.1. Breast Cancer 12

        1.1.1. Breast cancer in India 12

        1.1.2. Molecular Classification of Breast Cancer 13

        1.1.3. The TNBC problem 14

    1.2. Tumor Microenvironment (TME) 15

    1.3. Tumor Infiltrating Lymphocytes (TILs) 17

    1.4. TILs Recruitment to TME 19

    1.5. The Proteasome Complex 21

    1.6. Immunoproteasome 22

        1.6.1. IP structure 22

        1.6.2. Catalytic subunits 23

        1.6.3. Enzymatic activity 23

        1.6.4. Previous Studies 24

        1.6.5. Relationship to Tumor-Infiltrating Lymphocytes (TILs) 26

    1.7. Objective of the Study 28

2. Materials and Methods 29

    2.1. Sample Collection 29

2.2. Cohort Defining 29
2.3. Sectioning 30
2.4. Haematoxylin and Eosin Staining 30
2.5. Immunohistochemistry 31
2.6. Imaging 33
2.7. Scoring 34
2.7.1. H&E Scoring 34
2.7.2. IHC Scoring 35
2.8. Optimization of Antibody Dilutions 35
2.9. Antibody Selection 38
2.10. Statistical Analysis 39
3. Results 40
3.1. Breast Cancer Cohort Selection 40
3.2. Breast Cancer Cohort Characteristics 40
3.3. IP subunits correlation with TILs infiltration 42
3.4. IP subunits correlation with TILs infiltration across subtypes 43
3.5. Expression of LMP7 and PSMB10 across molecular subtypes 44
3.6. ROC analyses 45
3.7. IP subunit expression and response to NACT 46
3.8. IP subunit expression and patient survival outcomes 47
3.9. IP subunit expression and subtype-wise patient survival outcomes 50
4. Conclusion 52
5. Discussion 53
6. References 56

List of Tables

Table 1: Scoring scheme for IHC-stained samples/sections..... 35

Table 2: Ab information for IP subunits LMP7 (β5i), LMP2 (β1i) and PSMB10 (β2i). 36

Table 3: Demographic table showing clinical characteristics of IDC cohort patients 41

Table 4: Spearman's correlation analyses..... 42

List of Figures

Figure 1**:** Incidence and Mortality, Both sexes, in 2022 India vs World 12

Figure 2**:** Molecular classification of breast cancer 13

Figure 3**:** Survival curves for breast cancer subtypes at different stages 14

Figure 4**:** TME and different stages of cancer progression..... 15

Figure 5**.** TILs as a prognostic marker..... 18

Figure 6**:** Structure of the Proteasome complex 22

Figure 7**: Constitutive Proteasome and** Immunoproteasome..... 23

Figure 8**:** TCGA analysis of IP expression different tumour tissues..... 25

Figure 9**:** PSMB8 and PSMB9 overexpression and Cell compositions..... 26

Figure 10**:** Anti-tumor immunity supported by immunoproteasome 27

Figure 11: H&E images of a sample 31

Figure 12: IHC images of serial sections of a sample 33

Figure 13: Guidelines showing scoring for TILs as percentages. 34

Figure 14: LMP7 standardization. 36

Figure 15: LMP2 standardization 37

Figure 16:: PSMB10 standardization..... 37

Figure 17: Comparison of LMP2, LMP7 and PSMB10 expression. 38

Figure 18: Cohort selection process..... 40

Figure 19: Heatmap: spearman's r between IP subunits and %TILs score. 43

Figure 20: Heatmap: spearman's r between IP subunits and %TILs (subtypes) 44

Figure 21: LMP7 and PSMB10 expression in tumor and TILs across subtypes. 45

Figure 22 : ROC curves 46

Figure 23: pCR and RD for high vs low IP subunit expression..... 47

Figure 24: DFS and OS for IP in tumor 48

Figure 25: DFS and OS for IP in TILs..... 49

Figure 26: DFS and OS for IP in tumor across molecular subtypes 50

Figure 27: DFS and OS for IP in TILs across molecular subtypes 51

Figure 28: Relation between IP, TILs, and patient prognosis..... 55

Abstract

The proteasome system is the central proteolytic system of eukaryotic cells and is crucial for maintaining protein homeostasis by degrading misfolded or unwanted proteins into smaller peptides. Immunoproteasomes, which are specialized proteasomal complexes, enhance antigen processing for MHC class I presentation, influencing T cell-mediated responses. IP is predominantly found in immune cells and can be induced in non-immune cells by IFN-γ and TNF-α.

The Immunoproteasome complex has three active subunits in the catalytic core- β5i, β1i and β2i. The difference in constitutive proteasome and immunoproteasome catalytic activities is the enhanced chymotrypsin-like activity of the IP subunits, which in the tumor microenvironment helps shape the repertoire of neo-antigens. So, the immunoproteasome is involved in the modulation of chronic inflammatory environments, as well as in optimal antigen presentation of tumor epitopes to the tumor-infiltrating CD8+ T cells.

However, their expression in the tumor and tumor-infiltrating lymphocytes (TILs) and its relationship with TILs remain poorly understood in breast cancer.

Using immunohistochemistry, we found that LMP7(β5i) and PSMB10 (β2i) expression in tumor had a significant positive correlation, suggesting co-regulation. Moreover, high IP subunit expression in tumor negatively correlated with the TILs infiltration. We also saw a negative association of IP subunit expression with the prognosis of the patient.

A previous study on TILs had reported that a higher TILs score corresponded to better survival of the patient. Our study matches with this result in the sense that higher IP expression would lead to less immune infiltration and poor prognosis, and less immune infiltration would also lead to a poor prognosis, thereby establishing a concordance with the study.

Acknowledgments

I would like to express my heartfelt gratitude to my advisor, Dr. Madhura Kulkarni, for her invaluable guidance, encouragement, and unwavering support throughout my research. Her expertise and insights have been instrumental in shaping this work, and I am deeply grateful for her patience, belief in me, and mentorship. I truly could not have done this without her.

I extend my sincere thanks to Dr. Satyajit Rath, my expert on the TAC, for his invaluable advice and constructive feedback, which helped refine my approach and strengthen my work.

A special thank you to my once-mentors, Pooja and Gomathi, for teaching me the ways of the lab and setting the foundation for my learning. I am incredibly grateful to my labmates—Jisha, Sakshi, Manav, Disha, Anuvind, Smera, Khushi, and Malavika—for making the lab experience not just enriching but also immensely fun.

I would especially like to express my deepest gratitude to Bhavesh and Vedant for being my constants through every up and down, and for all the fun trips and memories we've shared. Their friendship and support have meant the world to me.

To Jassi and all my friends, thank you for always being there for me and lifting me up when I needed it the most.

And last, to Aai, Baba, and Vaishnav— thank you for being my pillars of strength and my unwavering support system. I owe everything to you.

Thank you, everyone.

Contributions

Contributor name	Contributor role
Sampada Ghute, Disha Kshirsagar, Dr. Madhura Kulkarni, Dr. Sabarinathan Radhakrishnan	Conceptualization Ideas
Sampada Ghute	Methodology
Sampada Ghute	Software
Dr. Madhura Kulkarni	Validation
Sampada Ghute	Formal analysis
Sampada Ghute	Investigation
Dr. Madhura Kulkarni, Dr. Sabarinathan Radhakrishnan	Resources
Sampada Ghute, Dr. Madhura Kulkarni	Data Curation
Sampada Ghute	Writing - original draft preparation
Dr. Madhura Kulkarni, Sampada Ghute	Writing - review and editing
Sampada Ghute	Visualization
Dr. Madhura Kulkarni	Supervision
Dr. Madhura Kulkarni	Project administration
Dr. Madhura Kulkarni	Funding acquisition

1. Introduction

1.1. Breast Cancer

Cancer is a group of diseases characterized by uncontrolled cell growth and division, often leading to the formation of malignant tumors. It may occur in any tissue or organ of the body and results from mutations that disrupt normal cellular processes.

1.1.1. Breast cancer in India

According to GLOBOCAN '22, after lung cancer, breast cancer is the second most prevalent cancer and the fourth highest cause of cancer-related deaths. The incidence and death rate in India is higher as compared to the Western population. Worldwide, breast cancer accounts for 11.5% of all cancer cases and 6.8% of cancer-related deaths. In India, it accounts for 13.6% of the total cases and 10.7% of cancer-related deaths *(Fig 1).*

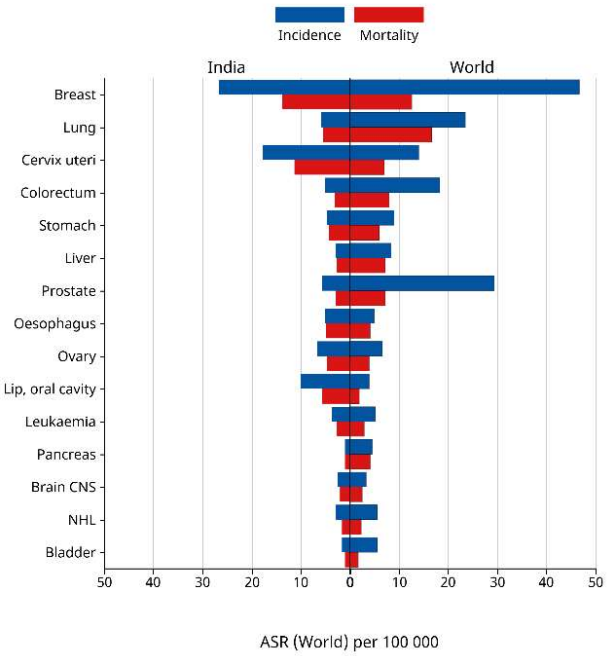

Figure 1: Age-Standardized Rate (World) per 100 000, Incidence and Mortality, Both sexes, in 2022 India vs World. Data from Globocan 2022

1.1.2. Molecular Classification of Breast Cancer

Breast cancer is a very heterogeneous disease. Hence, attempts are made to categorize breast tumors into different types based on morphology, molecular characteristics, receptor status, and genetic profile to help in diagnosis, prognosis, and treatment strategies.

Clinico-pathological and molecular features are used to classify breast tumors to prognosticate appropriate therapy. Several predictive and prognostic factors are used to classify breast tumors into various subtypes to ensure the therapy is matched to the patient's needs (Masood, 2016).

Breast cancers are classified into four molecular sub-types based on the immunohistochemical expression of the hormone receptors: estrogen (ER) and progesterone receptors (PR), and human epidermal growth factor receptor 2 (HER2). These are Luminal A (ER/PR+, HER2-), Luminal B (ER/PR+, HER2+), HER2 positive (ER-, PR-, HER2+), and Triple-negative breast cancer—TNBC (ER-, PR-, HER2-) *(Fig. 2).*

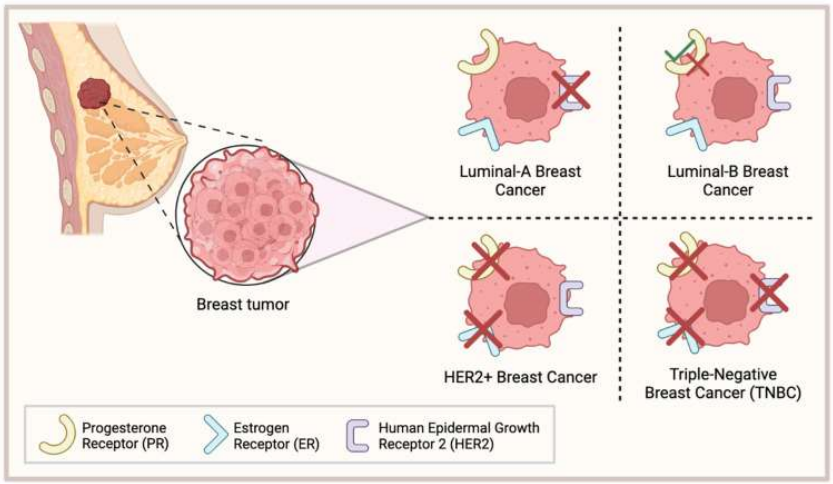

Figure 2: Molecular classification of breast cancer according to expression of surface receptors (Kirkby et al., 2023)

1.1.3. The TNBC problem

Triple-negative breast cancer (TNBC) has been categorized as a heterogeneous and aggressive type of breast cancer as this subtype of breast cancer tends to have onset at a younger age, higher mean tumour size, higher-grade tumours, and sometimes, a higher rate of node positivity. Combined with the lack of targetable receptors, the treatment of triple-negative breast cancer becomes challenging. TNBC is also associated with a higher risk of recurrence and poor prognosis than other subtypes. This calls for a need to identify prognostic markers that are predictive of patient outcomes and their response to therapies. *(Fig 3)* shows association between long-term survival and breast cancer subtypes at different cancer stages (Howlader et al., 2018).

In India, the prevalence of TNBC is much higher (24-31%) (Kulkarni et al., 2020) than in the Western population (12.2-13%) (Plasilova et al., 2016)

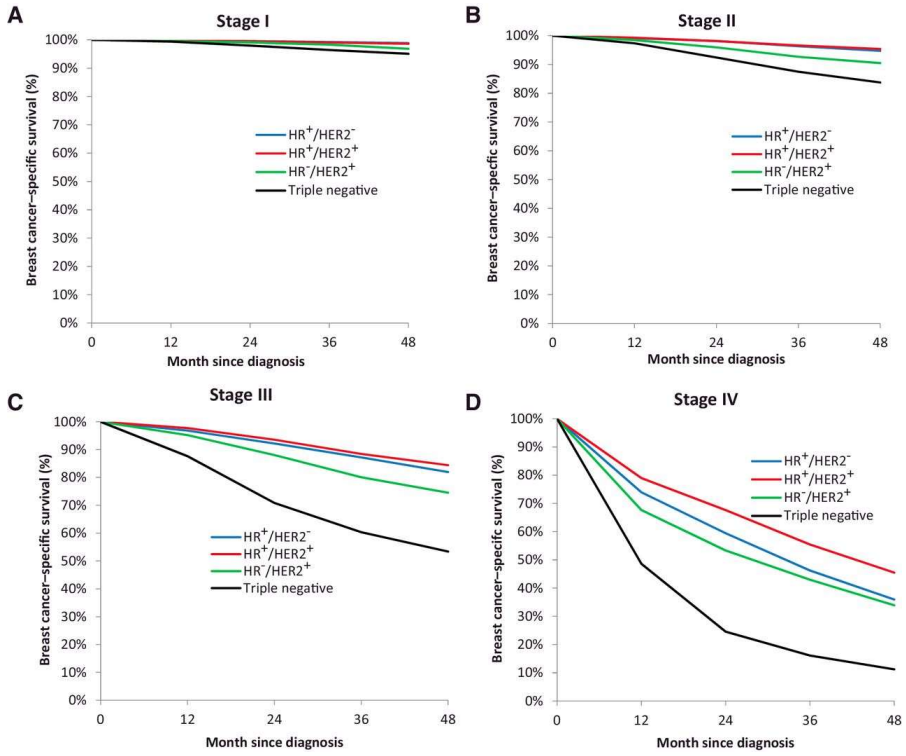

Figure 3: Survival curves for HR+/HER2-, HR+/HER2+, HR-/HER2+, and Triple negative breast cancers at Stage I, II, III, and IV. (Howlader et al., 2018).

1.2. Tumor Microenvironment (TME)

Cancer is a complex ecosystem rather than just a genetic disease and involves a range of non-cancerous cells and their various interactions within the tumor.

For cancer initiation and progression, genetic alterations are necessary, but they are not sufficient alone. Examinations of solid tumors have revealed that cancer is intricately complex and that the tumor microenvironment (TME) is a highly structured environment comprising cancer cells and diverse non-malignant cells surrounding them. These are collectively embedded in an extracellular matrix (ECM)(Yuan et al., 2023).

TME consists of tumor cells, stromal cells, a rich diversity of immune cells like microglia, macrophages and lymphocytes, cancer-associated fibroblasts (CAFs), endothelial cells, adipocytes, and non-cellular components of the ECM like collagen and fibronectin. The TME also contains a complex network of cytokines, chemokines, inflammatory mediators and matrix remodelling enzymes that serve as a source of intercellular communication *(Fig. 4).* (Balkwill et al., 2012)

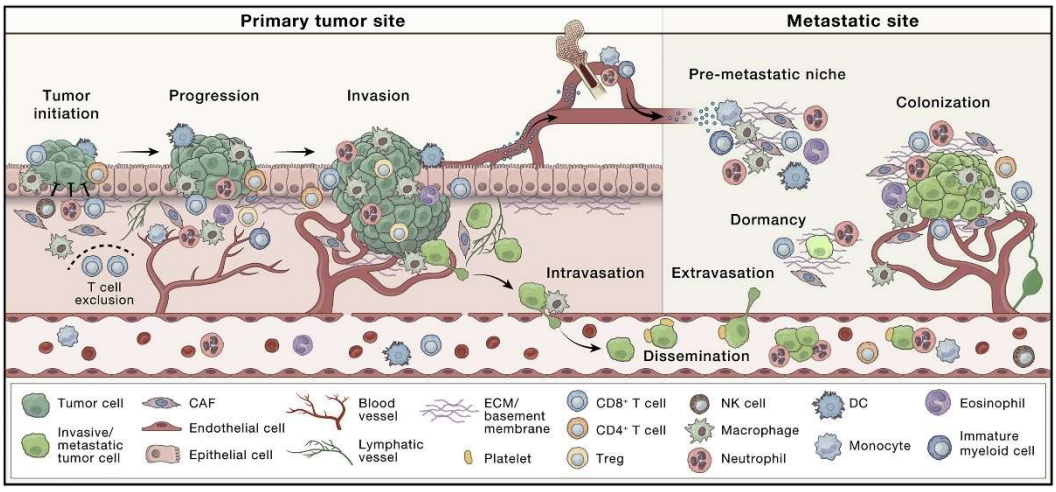

Figure 4: Tumor microenvironment (TME) and various cell types during different stages of cancer progression(de Visser & Joyce, 2023).

Studies in tumor biology have shown that the interactions and multiple exchanges between the tumor cells and their neighbouring tumor microenvironment also control tumor growth, cancer heterogeneity, epithelial-to-mesenchymal transition (EMT), migration, invasion, metastasis, vascularization, apoptosis, and chemotherapeutic drug resistance (Quail & Joyce, 2013).

Apart from the intrinsic features of the cancer cells, tumor stage, and patient characteristics, the cellular and functional state of the TME also differs depending on the organ site where the tumor arises. Various cells and their activities in the TME can be either pro-tumor (tumor supporting) or anti-tumor (tumor suppressive). Since the cells in TME and their secreted molecules play a critical role in the pathogenesis of cancer, they represent attractive therapeutic targets.

1.3. Tumor Infiltrating Lymphocytes (TILs)

The TME comprises of a range of immune cells, a significant part of which are tumor infiltrating lymphocytes (TILs). TILs mainly consist of T-cells and B-cell.

The interactions between tumor cells and the TME begin at the early stages of tumor formation and they both contribute to each other's dynamic changes (Ungefroren et al., 2011). Clinically, these interactions are important for evaluating cancer outcomes and the risk of progression, which is influenced by the characteristics of the TME, TILs, and the tumor.

The presence of TILs within the tumor serves as an indicator of the effectiveness of anti-cancer therapies like immune checkpoint inhibitors (ICIs) and neoadjuvant chemotherapy (NACT). Higher levels of tumor-infiltrating lymphocytes (TILs) in pre-treatment biopsies are associated with increased pathological complete response (pCR) rates to neoadjuvant chemotherapy (NACT) in breast cancer (BARROSO-SOUSA et al., 2024; Hong et al., 2021). A systematic review and meta-analysis found that elevated TILs correlated with higher pCR rates, particularly in triple-negative and HER2-positive breast cancer subtypes (Gao et al., 2020). This suggests that TILs can serve as predictive biomarkers for NACT efficacy in these breast cancer subtypes.

TILs are also the basis of CAR-T cell therapy, where TILs are harvested, cultured and amplified in vitro and infused back into the patient (Zhu et al., 2023).

Different lymphocytes act differently in the TME. For example, the subgroups of T lymphocytes show different activities against the tumor cells, affecting patient prognosis.

Recent studies in breast cancer have shown that TILs present in the tumour can predict response to therapies and the prognosis of the patient. Along with the amount of lymphocytic infiltrates, the phenotypes of these infiltrates also determine the clinical outcomes. CD8+ cytotoxic T-cells (CTLs) are essential for tumor destruction; hence they have an anti-tumor activity, and their high infiltration in the tumor is considered as a positive prognostic marker in cancers such as breast and ovarian cancers (Fanale et al., 2022; Liu et al., 2012). CD4+ T-helper 1 (Th1) cells help in antigen presentation through cytokine secretion and activation of antigen-presenting cells (APCs). In

contrast, Th2 cells, including CD4+ regulatory T-cells (Tregs), are responsible for promoting tumor growth and progression as they inhibit CTL function and promote anti-inflammatory immune responses and are therefore considered a predictor of poor prognosis for patients. (Frankowska et al., 2023)

So, it can be said that the predictive properties of a type of immune cell are not always homogenous, and different trends can be observed in different cancer types.

(Fig. 5A) shows that in a study on breast cancer patients in an Indian cohort by (Vaid et al., 2022), patients with TNBC had higher TILs infiltration than patients with HER2+ or ER+ breast cancers. The study also showed that a higher proportion of breast cancer patients with high TILs had better pCR rates than patients with low TILs *(Fig. 5B, C, D, E)*. A similar trend was observed by (Denkert et al., 2018) *(Fig. 5F)*.

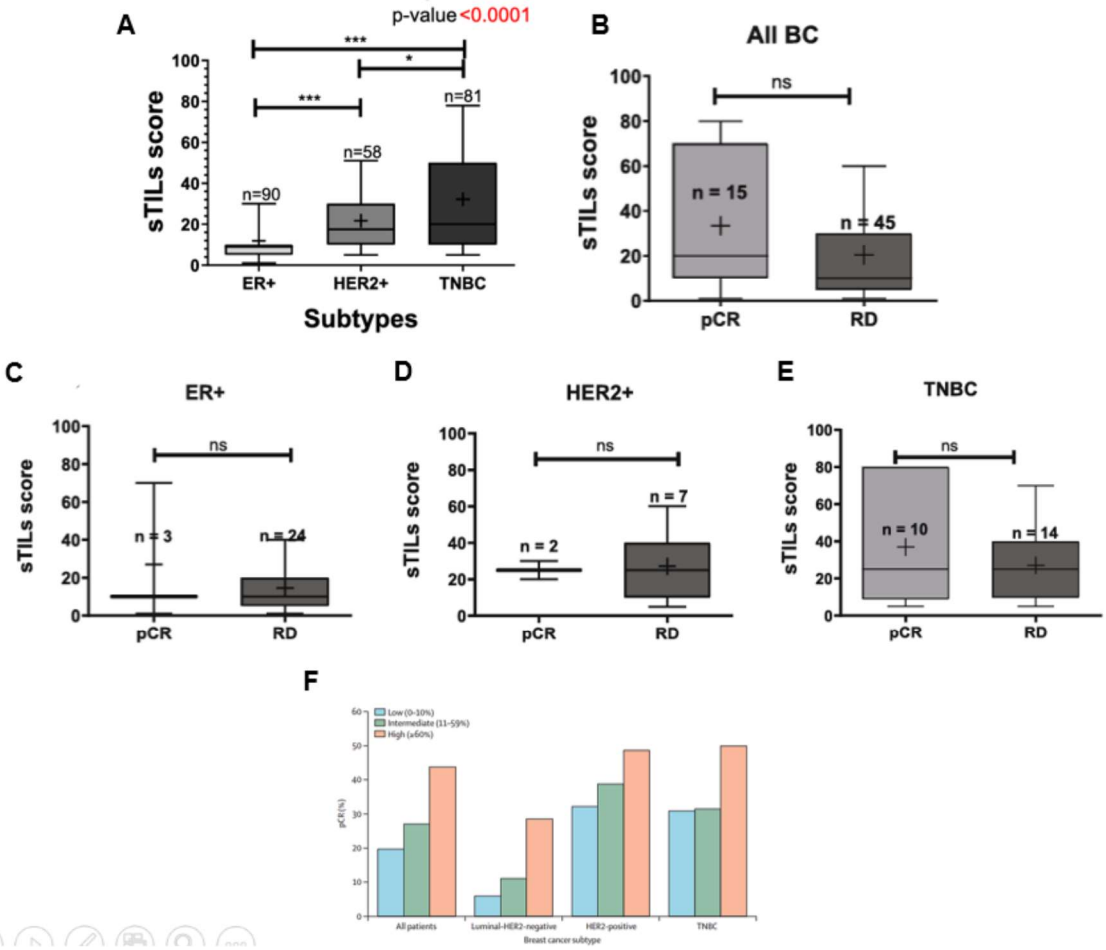

Figure 5. (A) TILs distribution across ER+, HER2+, TNBC breast cancer subtypes, (B) TILs distribution for patients with pCR and RD after NACT, (C, D, E) TILs distribution for pCR and RD across subtypes (Vaid et al., 2022), (F) % patients with pCR for different TILs distribution across subtypes (Denkert et al., 2018).

1.4. TILs Recruitment to TME

The recruitment of TILs to the TME is a highly coordinated process driven by various complex interactions involving tumor cells, stromal cells, chemokines, immune mediators, extracellular matrix (ECM) and tumor vasculature.

The primary catalyst for lymphocyte infiltration is the expression of antigens on the surface of tumor cells. Tumor cells also express some cytokines like VEGF, TGF-β, and TNF-α. Pro-inflammatory chemokines in the TME can also be altered to prevent T cell infiltration (Yang et al., 2024a).

Tumor cells can also modulate T cell infiltration by selective upregulation of specific genes like TGFB1, CTGF, and BHLH-E40 (Li et al., 2017). that respond to TGF-β, which initiates the epithelial-mesenchymal transition (EMT) through the TGF-β pathway. EMT then inhibits T-cell infiltration and upregulates immunosuppressive cytokines (Yang et al., 2024b). TGF-β promotes the expansion and activation of CAFs, which generate a dense extracellular matrix (ECM) that physically traps T cells in the stroma, preventing them from migrating towards the tumor regions. Excessive collagen deposition may also act as a barrier to T cell entry (Milosevic & Östman, 2024)

As the progression of solid tumors occur, large areas become deprived of oxygen, creating areas of hypoxia and necrosis which have limited nutrient availability. This imposes significant bioenergetic constraints on both tumor and immune cells. In such harsh conditions, tumor cells are capable of undergoing dynamic metabolic reprogramming that helps them confer cell plasticity and enhance survival, while depriving immune cells of nutrients that are essential for their function and survival. This may lead to a reduction in the number of TILs (Wang et al., 2024).

The vasculature in the tumor often has irregular distribution, branching and hence blood flow. This leads to dysregulation of T cell movement, as well as the formation of varying perfusion and oxygen level regions (Magnussen & Mills, 2021). The nutrient and oxygen availability heterogeneity across spatial regions influences T cell entry, function, and survival.

The T-cell entry is majorly driven by the antigens that are expressed on the tumor cell surface. One of the key mechanisms for antigen representation involves the

proteasome, a protein complex responsible for degrading intracellular proteins into peptides. These peptides are then loaded onto MHC class I molecules for presentation to cytotoxic T cells (CD8+ T cells), which are a significant component of TILs (Rana et al., 2024). In the context of an immune response, the standard proteasome can be replaced by the immunoproteasome, a specialized form that enhances antigen processing for MHC class I presentation. This shift is often induced by inflammatory cytokines such as IFN-γ, which are produced by activated TILs (Leister et al., 2022).

1.5. The Proteasome Complex

Protein turnover is essential for regulating protein levels and maintaining cellular integrity. A major enzyme involved in protein turnover regulation is the proteasome.

The proteasome system is the central proteolytic system of eukaryotic cells. It is a vital component of the ubiquitin-proteasome system (UPS) that maintains protein homeostasis by degrading unwanted or misfolded proteins into smaller peptides.

It is also a crucial component in the immunological surveillance of infected or cancerous cells, regulation of cell differentiation, cell-cycle progression and apoptosis (Vigneron & Van den Eynde, 2014).

The proteasome is made up of two subcomplexes– one 20S catalytic core and two terminal 19S regulatory particles. 20S proteasome can exist in several isoforms or subtypes, resulting in different catalytic activities. According to these differences, different types of proteasomes exist: Standard proteasome, Immunoproteasome, Intermediate proteasome, Thymoproteasome, and Spermatoproteasome (Abi Habib et al., 2022).

Out of these proteasome types, the Immunoproteasome is of particular interest in cancer research as it plays a role in modulating the immune responses in the tumor microenvironment.

1.6. Immunoproteasome

The immunoproteasome (IP) is constitutively expressed in immune cells such as T cells, B cells and antigen presenting cells (APCs). The assembly and expression of IP can be induced by proinflammatory cytokines, like interferon (IFN) γ, and tumour necrosis factor (TNF) α, or in response to stress conditions.

1.6.1. IP structure

The Immunoproteasome, like the constitutive proteasome, is made up of two subcomplexes– one 20S catalytic core and two terminal 19S regulatory particles. The 20S core is conserved among organisms and is a barrel-shaped particle made of four stacked heptameric rings – two α-rings and two β-rings. The two outer α-rings are identical and are composed of 7 α-subunits (α1–α7), while the two inner β-rings, also identical, comprise seven β-subunits (β1–β7) out of which three are catalytically active *(Fig. 6).*

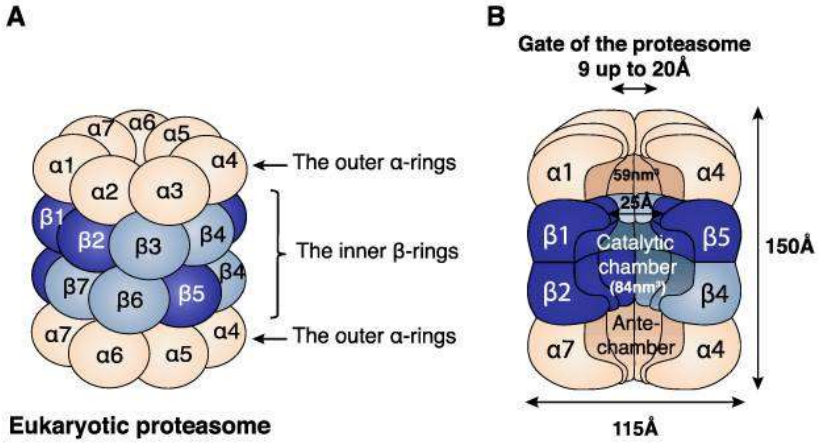

Figure 6: *Structure of the Proteasome complex (Abi Habib et al., 2022)*

The N-terminal regions of the α-subunits form gates that close the central pore, preventing unintended entry of substrates into the proteasome's internal chambers.

Protein hydrolysis inside the proteasome is carried out by the N-terminal threonines of three of the seven β-subunits, which have identical mechanisms for peptide bond hydrolyzation but different sequence specificity. This results in the proteasome having three different major proteolytic activities because of these three β-subunits. In CP (or SP), the catalytically active β-subunits which generate antigenic peptides are β1, β2 and β5. Whereas in IP, these are replaced by β1i (LMP2), β2i (MECL-1), and β5i (LMP7), respectively *(Fig. 7)*

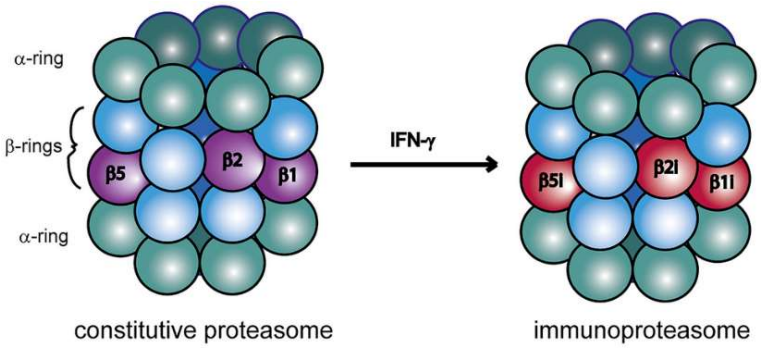

Figure 7**:** Replacement of CP subunits β1, β2 and β5 by subunits β1i, β2i and β5i to form Immunoproteasome (IP) (Leister et al., 2022)

1.6.2. Catalytic subunits

In humans, the genes encoding the subunits β1i and β5i are located on chromosome 6, and the gene encoding the subunit β2i is found on chromosome 16. The promoters of all these immuno-subunit genes have binding sites for the IFN regulatory factor (IRF)-1 transcription factor, which confers them responsiveness to IFN-γ.

1.6.3. Enzymatic activity

In the Constitutive proteasome, the three catalytic β-subunits, have distinct proteolytic activities – caspase-like (β1), trypsin-like (β2) and chymotrypsin-like (β5) activity. But in Immunoproteasome, β1i (LMP2), β2i (MECL-1), and β5i (LMP7) have chymotrypsin-

like, trypsin-like, and chymotrypsin-like activity respectively. This reduced caspase-like activity and enhanced chymotrypsin-like activity leads to more production of peptides with basic or hydrophobic C-termini, which are better suited for binding to MHC class I molecules. (Aki et al., 1994; Driscoll et al., 1993)

1.6.4. Previous Studies

Over the years, it has been established now that the Immunoproteasome is integral to immune regulation. For instance, studies have shown that the absence of IP subunits can impair the clearance of damaged proteins, leading to increased susceptibility to apoptosis under inflammatory conditions. (Kotamraju et al., 2003, 2006)

In Non-Small Cell Lung Cancer (NSCLC), the loss of immunoproteasome subunits was significantly associated with an advanced stage, recurrence, and metastasis. (Tripathi et al., 2016)

In a study by (Leister et al., 2021), upon TCGA data examination of melanoma patients, it was found that the high expression of the IP subunits LMP2, LMP7, and PSMB10 was significantly correlated with better overall survival of the patients.

Contrastingly, in a mice study by (Du et al., 2021), an inhibitor of LMP2 and LMP7 mitigated thrombocytopenia in passive murine Immune Thrombocytopenia (ITP) models.

In an analysis of the TCGA cohort by (Kumar et al., 2023), they saw how IP expression influenced patient survival in different cancer types *(Fig. 8).*

These findings suggest that immunoproteasome expression plays a significant role in modulating immune responses within the tumor microenvironment, influencing disease progression and patient prognosis across various cancers.

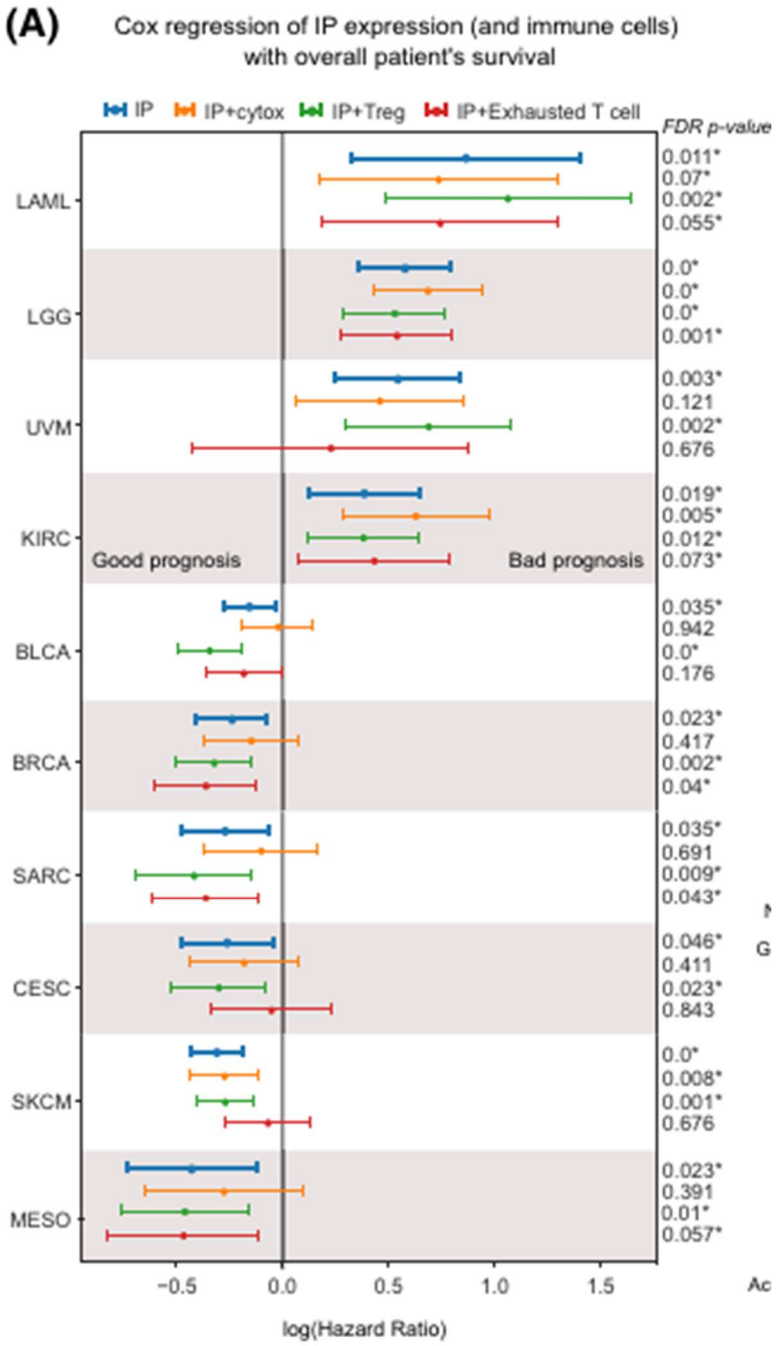

Figure 8: TCGA analysis of IP expression alone and combined with CTLs, T-reg cells and exhausted T-cells) in 10 different tumour tissues. (LAML-Acute myeloid leukaemia, LGG-Brain lower grade glioma, UVM-Uveal Melanoma, KIRC-Kidney renal clear cell carcinoma, BLCA-Bladder urothelial carcinoma, BRCA-Breast invasive carcinoma, SARC-Sarcoma, CESC-Cervical squamous cell carcinoma and endocervical adenocarcinoma, SKCM-Skin cutaneous melanoma, MESO-Mesothelioma)

1.6.5. Relationship to Tumor-Infiltrating Lymphocytes (TILs)

The Immunoproteasome's role in generating antigenic peptides is crucial for the activation and function of TILs. Efficient antigen presentation by tumor cells can enhance the recruitment and cytotoxic activity of TILs, leading to better tumor control. Conversely, impaired IP function may result in reduced antigen presentation, diminishing TIL efficacy and allowing tumor progression.

A study by (Kalaora et al., 2020) demonstrated that overexpression of IP subunits PSMB8 and PSMB9 showed significant positive association with infiltration of CD4+ and CD8+ cells, T-reg cells, NK cells and M1 macrophages (*Fig. 9).*

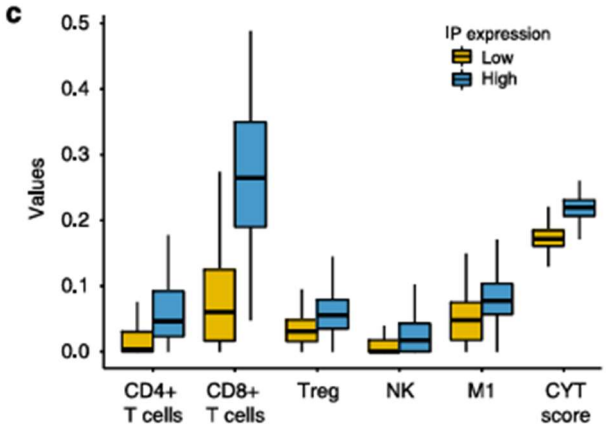

Figure 9: Association of PSMB8 and PSMB9 overexpression with Cell compositions characterized from patients' gene expression profiles

Another study by (Lee et al., 2019a) said that breast cancer tumors with high levels of LMP7 expression showed had more TILs in all subtypes.

Additionally, the immunoproteasome may influence the tumor microenvironment by modulating cytokine production and antigen presentation, thereby affecting the TILs' abundance and function. These findings underscore the critical relationship between immunoproteasome activity and TIL-mediated tumor immunity *(Fig. 10).*

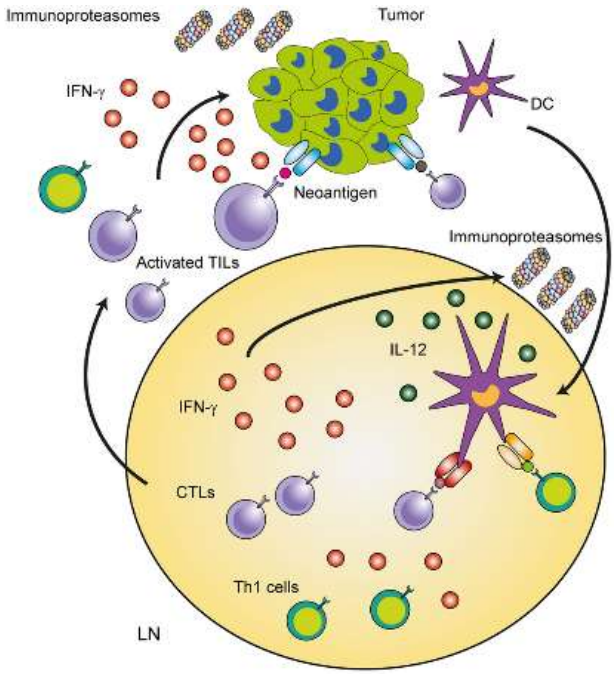

Figure 10: Anti-tumor immunity supported by immunoproteasome (Leister et al., 2022)

1.7. Objective of the Study

The objective of the study is to look at Immunoproteasome subunit differences in tumor and TILs in the tumor microenvironment. We will investigate if Immunoproteasome expression is associated with and can potentially predict immune cell infiltration. We will also see if Immunoproteasome from tumor or TILs is associated with patient prognosis.

2. Materials and Methods

2.1. Sample Collection

Patients who approach the Orchid Breast Health Clinic, Pune or associated clinics are registered in the patient database. Personal details, including data about medical and family history, are collected. The clinical data generated during/after the patient's treatment includes demography (age, menopausal status), medical data (radiology findings, biopsy and surgery histopathological exam findings including grade and TNM staging, and chemotherapy and radiotherapy details) and survival status (death, recurrence, follow-up data). All data is stored after de-identifying the patient's name. All patient samples sent to the pathology lab are formalin-fixed and paraffin-embedded, which prevents the decomposition of the tissue and fixes it at the point when it is collected. All the de-identified patient data, and the tissue samples in the form of FFPE blocks were received at IISER from PCCM.

2.2. Cohort Defining

The breast cancer tissue samples (in the form of FFPE blocks) and associated patient metadata are from the Prashanti Cancer Care Mission. The samples used for this study are from Indian patients; the non-Indian patient samples were excluded from the study. Also, the samples were from patients with Invasive Ductal Carcinoma (IDC). All Ductal carcinoma in situ (DCIS) and non-IDC samples were excluded from the study. All recurrence patient samples were also excluded. These samples were primary samples – meaning the patient had not undergone any treatment (mostly NACT or NAHT) until the collection of that sample. Samples for all subtypes – ER+, HER2+ and TNBC were included. The FFPE blocks which had less tissue or couldn't be sectioned were excluded from the cohort.

2.3. Sectioning

Breast cancer tissue samples from patients fixed as FFPE (Formalin fixed paraffin embedded) blocks were sectioned on the Microtome (Leica Microtome RM2255). 4-micron sections were taken and collected on positively charged slides (PathnSitu PS001), and stored at 4°C. For long term storage of the sections, the slides with sections were paraffin-coated before storing at 4°C.

2.4. Haematoxylin and Eosin Staining

Haematoxylin and Eosin (H&E) staining is a histological staining method that uses haematoxylin and eosin dye to differentiate cell types and visualize the tissue structure. The haematoxylin stains all the nuclei purple and the eosin stains all the cytoplasm and stroma pink (Fig. 11). In this study H&E was used to score for tumor and TILs present in the tissue.

Slides with tissue sections were deparaffinized in an oven at 62° C overnight, followed by xylene washes and serial rehydration (explained in the next section, 2.5.). The tissue was treated with Mayer's Haematoxylin dye for 15 minutes. Haematoxylin powder (Sigma Aldrich H3136-25G) was used to make Mayer's haematoxylin (recipe described in next section). After the Haematoxylin step, the tissue was given an acid wash (36% canc. HCL 4 mL and 95% ethanol 396 mL) followed by a running tap water bath. Next, the tissue was treated with Eosin dye (Sigma Aldrich Eosin Y E4009-5G) (1:1 dilution in 80%ethanol and 3-4 drops of GAA) for 1 minute followed by serial dehydration, xylene wash and mounting (described in next section).

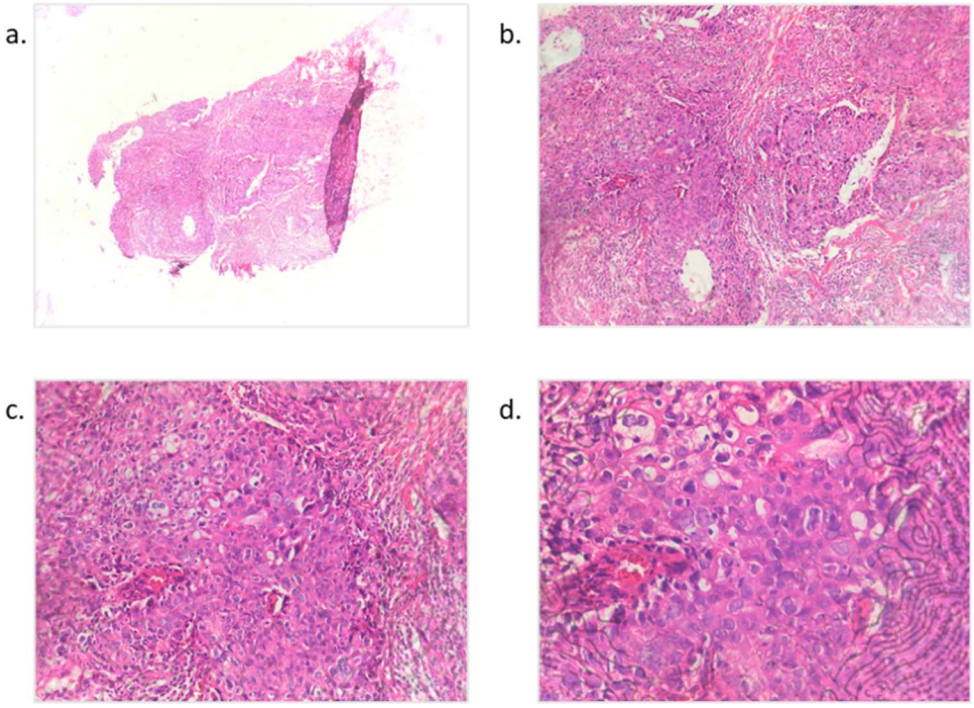

Figure 11: H&E images of a sample at a. 4X, b. 10X, c. 20X, and d. 40X magnifications. Haematoxylin stains all the nuclei blue, and eosin stains the cytoplasm and stroma pink. The larger epithelial cells with diffused and irregular sized nucleus are the tumor cells. The smaller, rounder and densely stained nuclei represent the TILs.

2.5. Immunohistochemistry

Slides with tissue sections were deparaffinized in an oven at 62° C overnight, followed by two 15-minute xylene washes. The tissue was then rehydrated using serially diluted ethanol washes (100%, 90%, 70% EtOH, followed by MQ). Next, the tissue was treated with an H2O2 block (UltraVision Hydrogen Peroxide Block- Epredia, TA-125-H2O2Q) for 30 minutes, followed by a 5-minute PBST wash. Peroxide blocking was done to inactivate all the endogenous peroxidases in the tissue. The slides were then kept in Tris-EDTA buffer (pH 9.0) and antigen retrieval was performed using the PathnSitu Multi Epitope Retrieval System to unmask all the antigenic epitopes. PBST wash was given after retrieval, and then the tissue was treated with Protein Block (UltraVision Protein Block- Epredia, TA-125-UB) for 30 minutes to reduce

unwanted background staining. After blocking, tissue was treated with 1° Ab (LMP7, LMP2 and PSMB10) (Table 2) diluted in antibody diluent (OP Quanto, Epredia, TA-125-ADQ) and kept at 4°C overnight.

Next, a PBST wash of 20 minutes was given, followed by treatment with 1° Ab Amplifier (Primary Antibody Amplifier Quanto- Epredia TL-125-QPB) for 10 minutes. 1° Ab amplifier is used to amplify the signal of the primary antibody. After a PBST wash of 20 minutes, Horseradish Peroxidase Polymer (HRP Polymer Quanto, TL-125-QPH), which conjugates to the 2° Ab, was administered to the tissue for 10 minutes, followed by another PBST wash of 20 minutes. DAB chromogen (UltraVision Quanto HRP DAB TA-125-QHDX) (30 µL DAB [TA-001-QHCX] in 1000 µL DAB Quanto Substrate [TA-125-QHSX]) was put on the tissue for a minute and transferred into tap water. The DAB and the HRP form a visible brown precipitate. Next, Mayer's haematoxylin was put on the tissue* as a counterstain, and the slides were kept in a water bath afterwards. This was followed by dehydration of the tissue by using serial dilutions of ethanol (70%, 90%, and 100%). The slides were kept to air dry and then given two 15-minute xylene washes. The slides were mounted with DPX (Qualigen, Q18404) and coverslips HiMedia BG013C)

**Two hematoxylin dyes were used for staining the samples:

1. Haematoxylin- Sigma Aldrich (H3136-25G) was used to make haematoxylin dye. To make 50 mL of Mayer's haematoxylin dye, 2.5g of potash alum, 50 mg of haematoxylin powder, 10 mg of sodium iodate and MQ to make up the volume to 50 mL was used. 1 mL of glacial acetic acid was added and the solution was filtered before use. The tissue was stained with this dye for 5 minutes.

2. Ready-to-use Haematoxylin Solution – Mayer's (SRL Diagnostics 48441) was used to stain the tissue for 10 minutes, followed by a running tap water bath of 10 minutes.

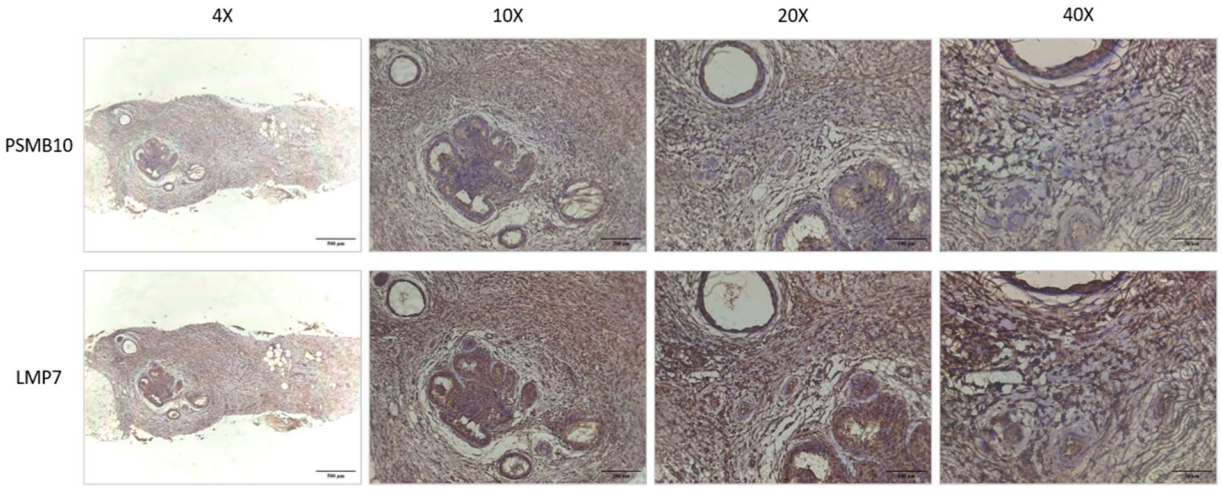

Figure 12: IHC images of serial sections of a sample at 4X, 10X, 20X, and 40X magnifications. Haematoxylin stains all the nuclei blue, and DAB forms a brown precipitate at the place of the target protein (PSMB10-top and LMP7-bottom panel). The larger epithelial cells with diffused and irregular sized nucleus are the tumor cells. The smaller, rounder and densely stained nuclei represent the TILs.

2.6. Imaging

The primary imaging of the IHC stained slides was done on the Mantra Brightfield Microscope (MN1707N0041 Perkin Elmer) and Mantra Snap 1.0 (Build 1.0.6045.14148, 2016 Perkin Elmer). Images of magnification 4X, 10X, 20X, and 40X were captured. Akoya Biosciences inForm software was used to convert .im3 format images from Mantra to .tiff images.

All the slides will be later sent to OptraSCAN India Pvt. Ltd. for whole slide scanning at 40X magnification.

2.7. Scoring

2.7.1. H&E Scoring

All H&E-stained samples were scored for tumor and TILs in percentages by a certified pathologist, Dr. Aniruddha. %Tumor is the percentage of total cells that are tumor cells, %TILs scoring is defined according to the linternational guidelines on TIL-assessment in breast cancer given by the International TILS Working Group *(Fig. 13)*

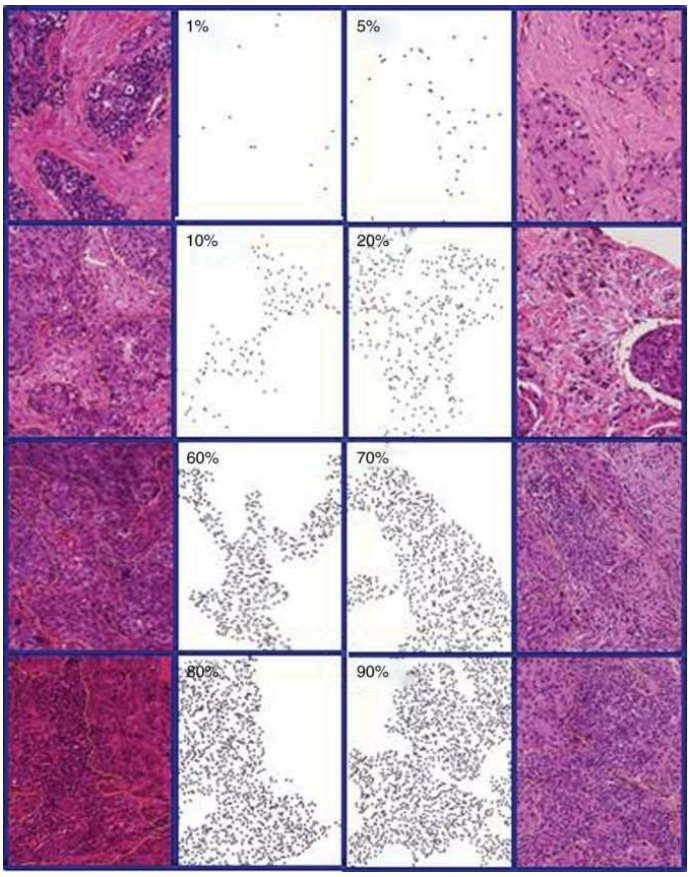

Figure 13: Guidelines showing scoring for TILs as percentages. The panels in the centre are graphics showing a similar TILs density in same ROI as the histological image. (Salgado et al., 2015)

2.7.2. IHC Scoring

IHC scoring for all the samples was done by Dr. Nutan Zumale. % expression of IP subunit and its intensity was scored. Intensity was coded as 0, 1, 2 and 3, where 0 means no expression, 1 is weak positive and 2 is strong positive. A composite score was calculated by first binning the % expression and assigning codes to the group, and then multiplying the binned %expression score and the intensity *(Table 1).* The % expression and intensity of the IP subunit was scored for in tumor and TILs separately.

% expression score	Binned % score	Intensity	Composite Score
0 1-10 11-40 >40	0 1 2 3	0: no expression 1: low expression 2: high expression	Binned % score × Intensity (0-6)

Table 1: Scoring scheme for IHC-stained samples/sections.

2.8. Optimization of Antibody Dilutions

We had 3 antibodies (abcam), Anti-Proteasome 20S LMP7 antibody [EPR14482(B)], Anti-Proteasome 20S LMP2 antibody [EPR22042], and Anti-PSMB10/MECL1 antibody [EPR14902], for the IP subunits β5i, β1i, and β2i respectively. The antibody dilutions suggested by abcam were 1:1700 for LMP7, 1:2000 for LMP2, and 1:100 for PSMB10, all in pH 9.0. The dilutions used for standardization for our experiments were 1:500 and 1:1000 for LMP7, 1:1000 and 1:2000 for LMP2, and 1:500 and 1:1000 for PSMB10 *(Table 2).*

For all the antibodies, lower dilutions showed better results (*Fig.14, 15, 16*) So, the dilutions finalized for the experimental study were 1:1000 for LMP7, 1: 2000 for LMP2, and 1:1000 for PSMB10.

Subunit	Proteasome subunit beta-5i	Proteasome subunit beta-1i	Proteasome subunit beta-2i
Antibody	Anti-Proteasome 20S LMP7 [EPR14482(B)]	Anti-Proteasome 20S LMP2 [EPR22042]	Anti-PSMB10/MECL1 [EPR14902]
Catalog no.	ab180606	ab242061	ab183506
Dilutions (suggested by abcam)	1/1700	1/2000	1/100
To test	1:1000 and 1:500	1:1000 and 1:2000	1:1000 and 1:5000
Antigen Retrieval Conditions	Perform heat mediated antigen retrieval with Tris/EDTA buffer pH 9.0	Perform heat mediated antigen retrieval with Tris/EDTA buffer pH 9.0	- Perform heat mediated antigen retrieval with Tris/EDTA buffer pH 9.0

Table 2: Table showing antibody information, abcam suggested Ab dilutions, and dilutions tested for standardization of antibodies for IP subunits LMP7 (β5i), LMP2 (β1i) and PSMB10 (β2i).

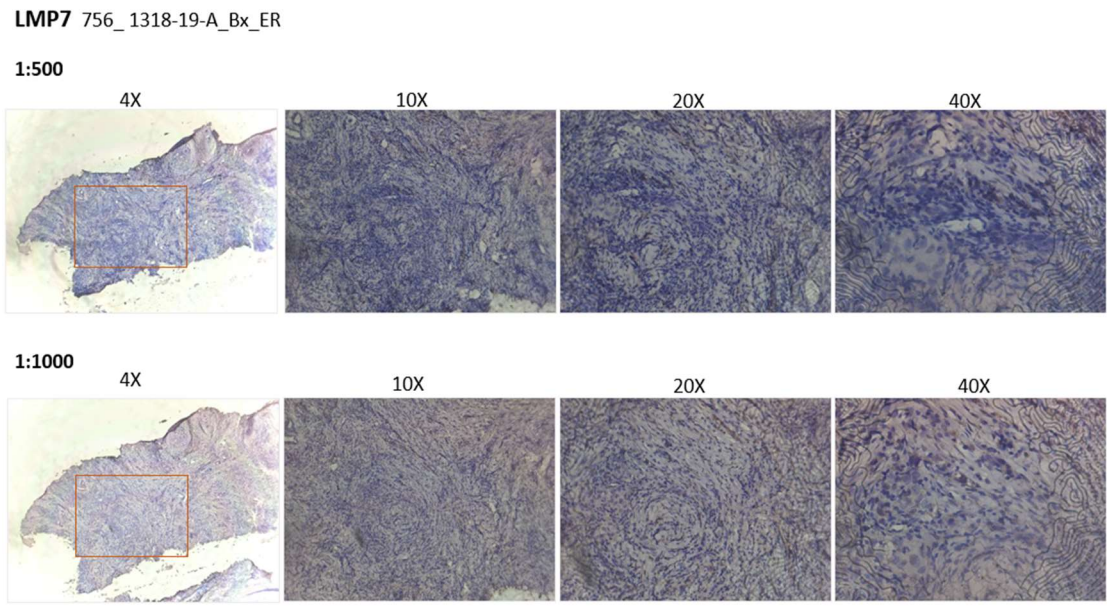

Figure 14: LMP7 (IP subunit β5i) expression in sample 756_ 1318-19-A_Bx_ER. Same ROI of two sections stained for LMP7 with 1:500 and 1: 1000 antibody dilutions respectively.

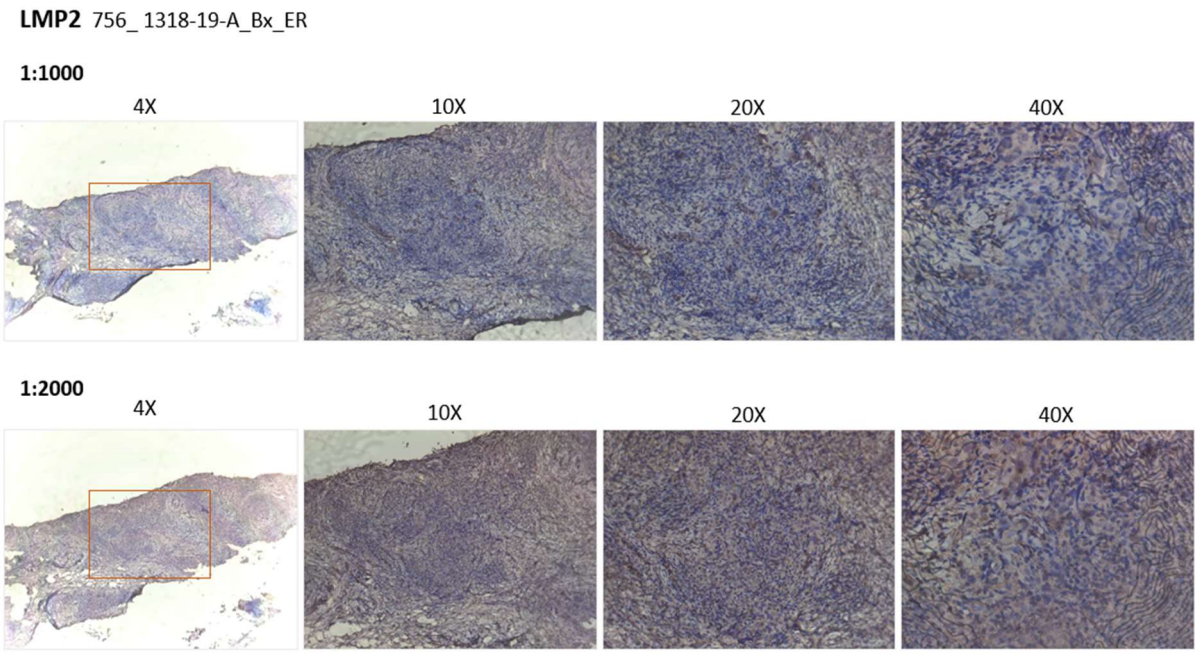

Figure 15: LMP2 (IP subunit β1i) expression in sample 756_ 1318-19-A_Bx_ER. Same ROI of two sections stained for LMP2 with 1:1000 and 1: 2000 antibody dilutions respectively.

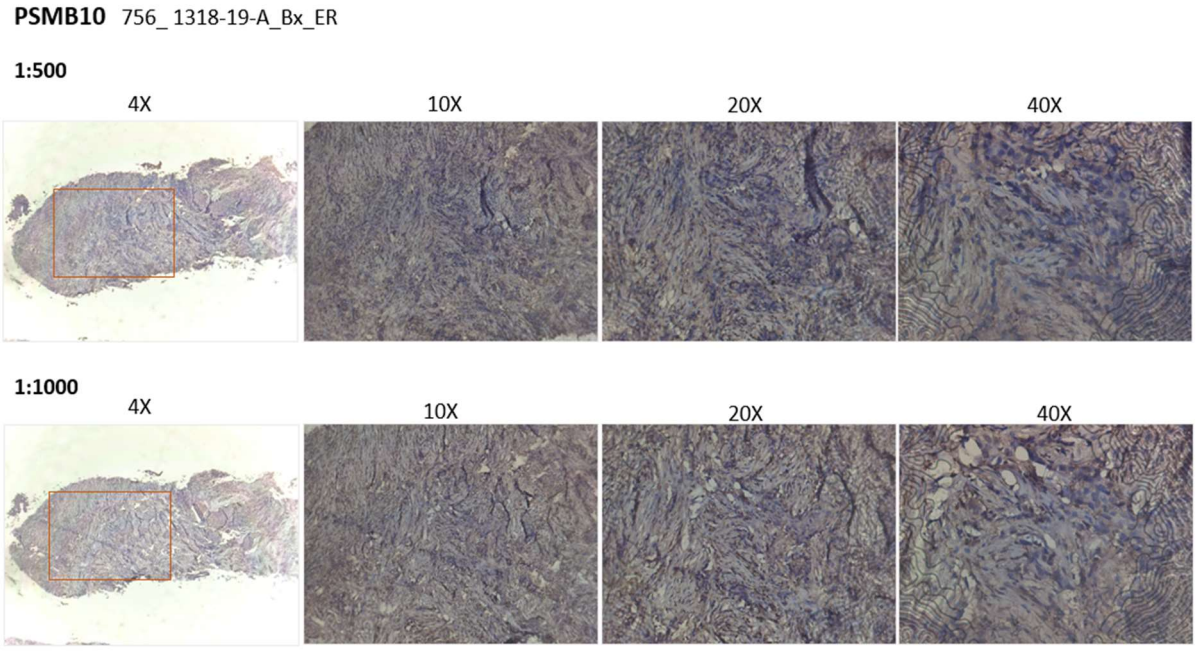

Figure 16:: PSMB10 (IP subunit β2i) expression in sample 756_ 1318-19-A_Bx_ER. Same ROI of two sections stained for PSMB10 with 1:500 and 1: 1000 antibody dilutions respectively.

2.9. Antibody Selection

Upon preliminary observations, out of the 3 catalytic subunits, the expression of LMP2 (β1i) subunit, and LMP7 (β5i) subunits were found to be similar *(Fig. 17*). LMP7 and LMP2 are also expressed on the same loci of chromosome 6, explaining the similar expression patterns (Monaco & McDevitt, 1986). Therefore, LMP7 and PSMB10 were taken forward for the study as it also helped save the patient samples.

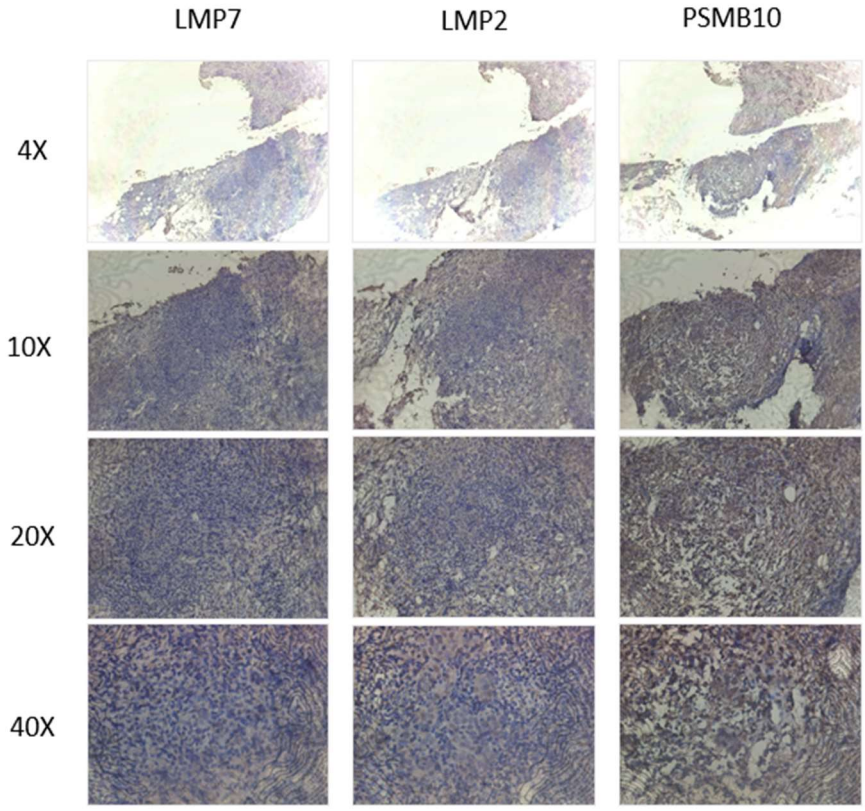

Figure 17: Comparison of LMP7 and PSMB10 expression. Three serial sections of the same breast cancer sample were IHC stained with antibodies for all three IP subunits. Same ROI for the samples shows that expression of LMP7 and LMP2 was very similar and that of PSMB10 was different.

2.10. Statistical Analysis

All statistical analysis was done using GraphPad Prism v.5. and IBM SPSS v.30.) Chi-square contingency test was used for the demographic table. One-way ANOVAs were done to test the statistical significance for differences in mean expression of IP. Kaplan-Meier graphs were plotted for overall survival (OS) and disease-free survival (DFS) curves.

3. Results

3.1. Breast Cancer Cohort Selection

The primary cohort for this study included 232 IDC patient samples for which H&E data was available (%tumor and %TILs score). Out of these 232, there were 92 samples which had very less or no tissue on the FFPE block, or there were no extra sections for the tissue. 2 samples were recurrence biopsies, which were excluded from the study as they are not primary tissue. The FFPE block details were not available for one sample, and 2 samples were later found to be DCIS (ductal carcinoma in situ). Therefore, the final sample number came down to 135 (57 ER+, 34 HER2+, and 44 TNBC samples) *(Fig. 18).*

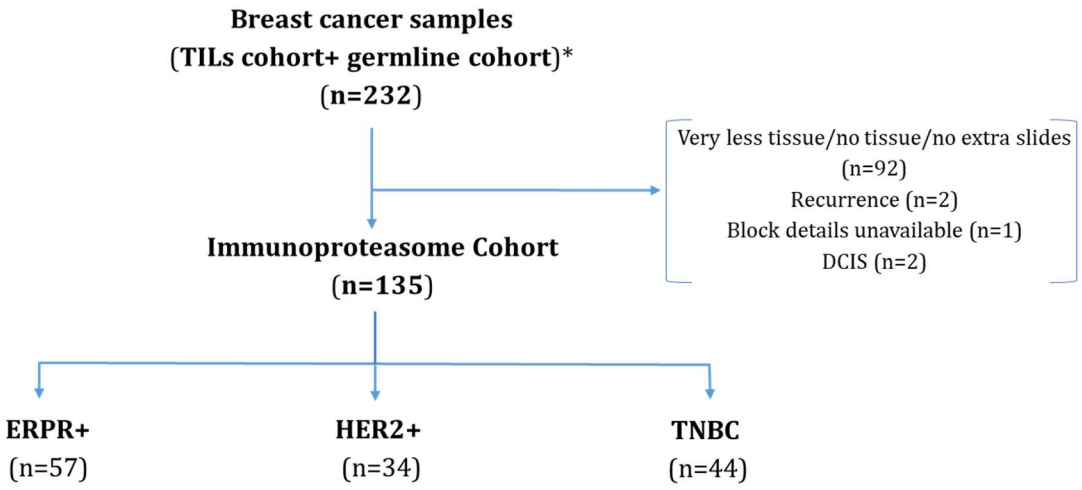

Figure 18: Flow chart representing the cohort selection process

3.2. Breast Cancer Cohort Characteristics

135 primary breast cancer tissue samples of Indian patients from PCCM were taken for the study. All samples were IDC. The demographic data and clinical characteristics of these patients are given in (*Table 3)*. according to their molecular subtypes. The range of age of the patients in the cohort is 28 to 86 years, and the average age at diagnosis is 55.23 years. Out of the 135 patients, 66.93% patients were presented at

a later stage and 33.06% at an early stage. Similarly, a majority of the patients (73.04%) were post-menopausal and 26.96% were pre-menopausal. 65.60% patients across the molecular subtypes had a low tumor grade (I/II) and 34.40% had high tumor grade (III/IV). But the incidence of higher tumor grade was significantly more in patients with TNBC (19.20%) than ER+ or HER2+ breast cancer (8.80% and 6.40% respectively). The pathological tumor size, lymph node positivity, clinical and pathological stage did not have much difference across the subtypes. Out of the total 135 patients in the cohort 30.95% (n=39) patients underwent neoadjuvant chemotherapy (NACT). The patients who received neoadjuvant hormonal therapy (NAHT) were also included in this category. 81.25% of the patients who had undergone NACT had residual disease (RD) and only 18.75% showed pathological complete response (pCR).

No. of patients		All cohort	ER+	HER2+	TNBC	p-values
		135	57	34	44	
Age (n=124)+A3:F27	(Mean ± S.D)	55.226 ± 12.44	56.667 ± 12.53	54.654 ± 12.49	53.585 ± 12.58	
	Early (<50)	33.06% (41)	13.71% (17)	6.45% (8)	12.90% (16)	0.6095
	Late (≥ 50)	66.93% (83)	32.26% (40)	14.52% (18)	20.16% (25)	
Menopausal status (n=115)	Pre	26.96% (31)	13.91% (16)	2.61% (3)	10.43% (12)	0.181
	Post	73.04% (84)	33.91% (39)	18.26% (21)	20.87% (24)	
Grade (n=125)	Low (I/II)	65.60% (82)	36.00% (45)	14.4% (18)	15.20% (19)	0.0008
	High (III)	34.40% (43)	8.80% (11)	6.4% (8)	19.20% (24)	
Tumor size (cT) (n=120)	T1	30% (36)	15.00% (18)	5.00% (6)	10.00% (12)	0.9513
	T2	61.67% (74)	26.67% (32)	14.17% (17)	20.83% (25)	
	T3	6.67% (8)	3.33% (4)	0.83% (1)	2.50% (3)	
	T4	1.67% (2)	0.83% (1)	0	0.83% (1)	
LN status (cN) (n=117)	Negative	29.0% (34)	14.17% (17)	9.17% (11)	8.33% (10)	0.0973
	Positive	70.94% (83)	32.50% (39)	9.17% (11)	26.67% (32)	
Clinical Stage (n=135)	Early (<IIB)	54.07% (73)	20.69% (30)	11.72% (17)	17.93% (26)	0.0007
	Late (≥IIB)	33.33% (45)	17.24% (25)	3.45% (5)	10.34% (15)	
	NA	12.59% (17)	1.38% (2)	8.28% (12)	8.97% (3)	
pT (primary tissue, no NACT) (n=108)	T0	12.04% (13)	7.41% (8)	0	4.63% (5)	0.0511
	T1	23.15% (25)	9.26% (10)	3.70% (4)	10.19% (11)	
	T2	59.26% (64)	19.44% (21)	22.22% (24)	17.59% (19)	
	T3	2.78% (3)	2.78% (3)	0	0	
	T4	2.78% (3)	0.93% (1)	0.93% (1)	0.93% (1)	
pN (primary tissue, no NACT) (n=107)	Negative	63.35% (68)	21.50% (23)	16.82% (18)	25.23% (27)	0.0954
	Positive	36.45% (39)	18.69% (20)	10.28% (11)	7.48% (8)	
Pathological Stage (primary tissue, no NACT) (n= 92)	Early(<IIB)	88.04% (81)	32.61% (30)	23.91% (22)	31.52% (29)	0.0764
	Late(≥IIB)	11.96% (11)	8.70% (8)	1.09% (1)	2.17% (2)	
NACT (n=126)	No	69.05% (87)	21.43% (27)	23.81% (30)	23.81% (30)	<0.0001
	Yes	30.95% (39)	22.22% (28)	0	8.73% (11)	
PCR status after NACT (n= 32)	pCR	18.75% (6)	9.38% (3)	0	9.38% (3)	0.2717
	RD	81.25% (26)	59.38% (19)	0	21.88% (7)	

Table 3: Demographic table showing clinical characteristics of the IDC cohort patients according to the molecular subtypes (ER+, HER2+. TNBC). For pT, Tis (carcinoma in situ) was clubbed with T0. For pCR, 'Complete response with Tis' was considered under pCR.

3.3. IP subunits correlation with TILs infiltration

The composite score of the IP subunit LMP7 in tumor cells was found to be significantly correlated to the composite score of the PSMB10 subunit in tumor cells (*spearman's r 0.3652, p-value <0.0001*) *(Table 4)*. This means that in tumor cells, with increase in expression of one subunit, expression of the second unit may also increase. Their correlated expression could indicate that the tumor cells upregulate the entire immunoproteasome complex rather than individual subunits.

Similar results have been shown in a study by (Lee et al., 2019b) where they used TCGA data and found that LMP7 and PSMB10 expression had a significant positive correlation (*rho 0.822, p < 0.001)*.

However, LMP7 and PSMB10 in TILs did not show any significant correlation (*spearman's r 0.1182, p= 0.1737*).

		%TILs	Composite Score (LMP7-tumor)	Composite Score (LMP7-TILs)	Composite Score (PSMB10-tumor)	Composite Score (PSMB10-TILs)
%TILs	spearman's r		-0.2912	-0.07719	-0.2867	-0.01584
	p-value		0.0007	0.3772	0.0008	0.8564
Composite Score (LMP7-tumor)	spearman's r	-0.2912		0.3725	0.3652	
	p-value	0.0007		<0.0001	<0.0001	
Composite Score (LMP7-TILs)	spearman's r	-0.07719	0.3725			0.1182
	p-value	0.3772	<0.0001			0.1737
Composite Score (PSMB10-tumor)	spearman's r	-0.2867	0.3652			0.3414
	p-value	0.0008	<0.0001			<0.0001
Composite Score (PSMB10-TILs)	spearman's r	-0.01584		0.1182	0.3414	
	p-value	0.8564		0.1737	<0.0001	

Table 4: Spearman's correlation analyses performed using GraphPad Prism V.5.

Moreover, when expression of the two subunits was compared in tumor and TILs, the correlation was positive. LMP7 expression in tumor was positively correlated with LMP7 expression in TILs (*r 0.3725, p <0.0001).*

Similar results were seen for PSMB10 expression also *(Table 4).* This observation could mean that the IP expression in TILs or tumor facilitates its expression in the other like in a feed-forward loop.

The composite score of LMP7 subunit in tumor was negatively correlated with the %TILs score (TILs scoring described in Methods section (*r -0.2912, p=0.0007*). The same trend was followed by PSMB10 in tumor, where the negative correlation was significant (*r -0.2867, p=0.0008*).

This result shows that high expression of IP in the tumor could be leading to reduced lymphocyte infiltration in the tumor.

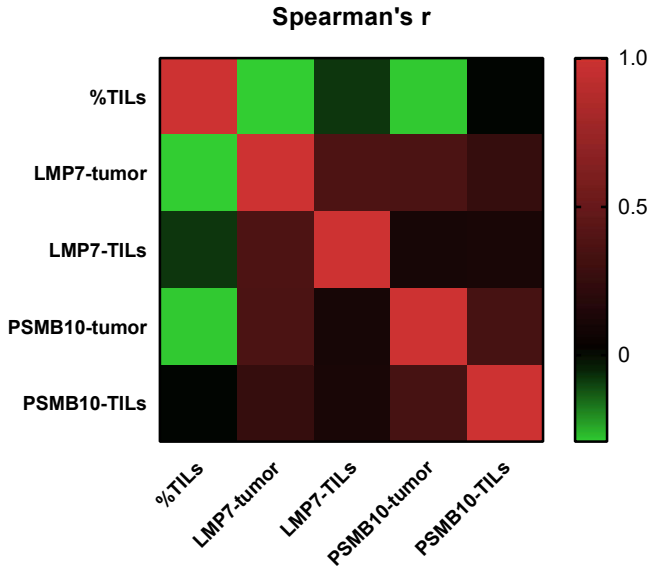

Figure 19: Heatmap representing spearman's correlations between IP subunits and %TILs score. Plotted using GraphPad Prism V.5.

3.4. IP subunits correlation with TILs infiltration across subtypes

When the correlations as given in section 3.3. were analysed for the breast cancer subtypes, similar results were observed *(Fig. 20*); though the significance was reduced due to a smaller number of samples in each subtype.

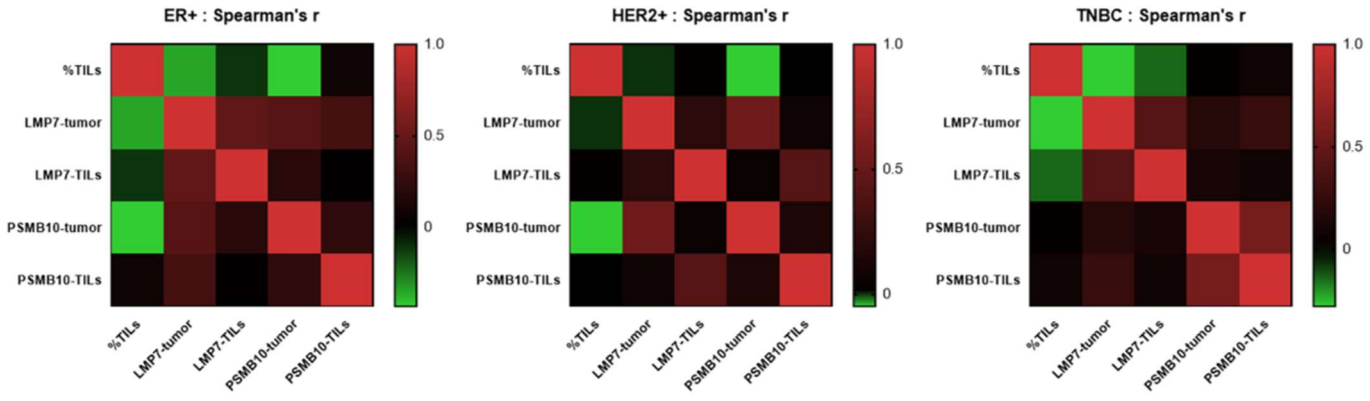

Figure 20: Heatmap representing spearman's correlations between IP subunits and %TILs score for ER+, HER2+, and TNBC. Plotted using GraphPad Prism V.5

3.5. Expression of LMP7 and PSMB10 across molecular subtypes

We also looked at the mean % expression and mean composite scores of the subunits in tumor for the subtypes ER+, HER2+, and TNBC and found that IP expression in tumor varied across the molecular subtypes, while its expression in TILs did not. For LMP7 in tumor, ER+ breast cancer had the highest mean % expression and mean composite score, followed by HER2+ and TNBC *(Fig. 21A, E).* For PSMB10 in tumor, HER2+ breast cancer had the highest mean % expression and mean composite score, followed by ER+ and TNBC *(Fig. 21B, F).* Mean % expression or mean composite score for LMP7 and PSMB10 in TILs showed no variation across the subtypes *(Fig. 21C, D, G, H).* This could be because Immunoproteasome is supposed to be expressed in immune cells, so the molecular subtype, which is defined by the kind of receptor that is preset on the tumor cell surface, would not matter.

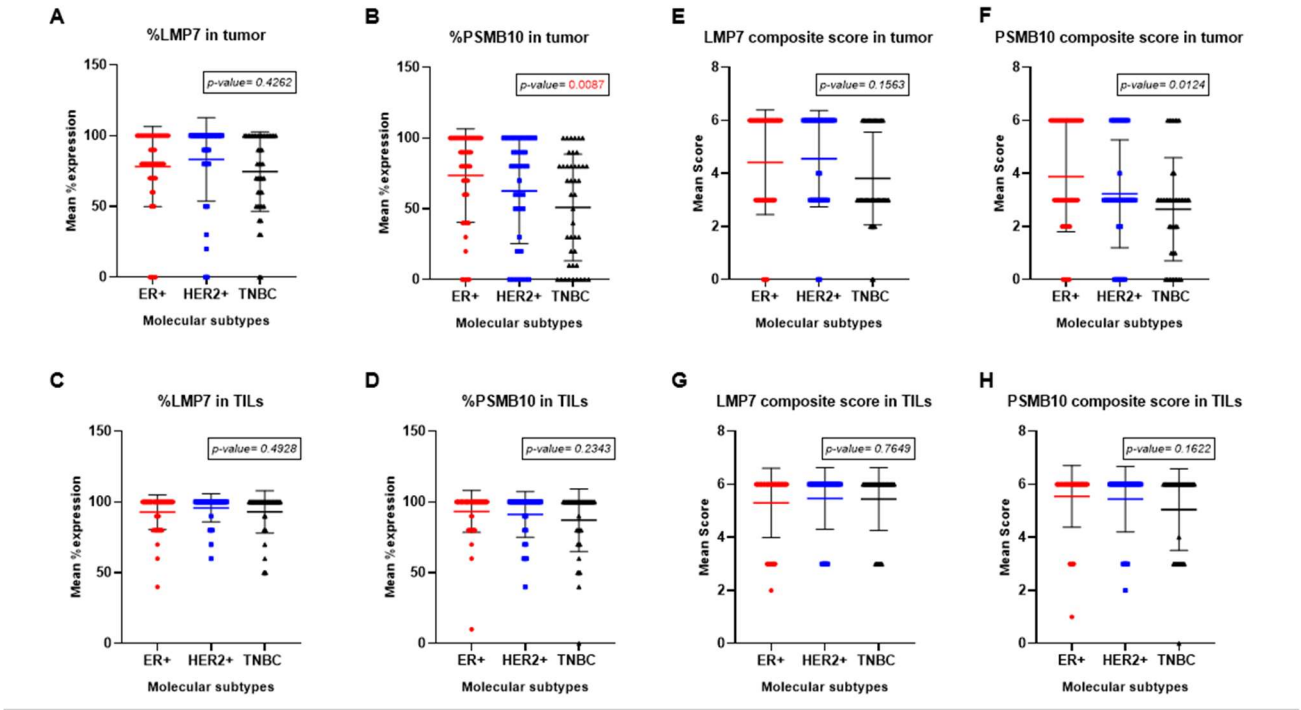

Figure 21: Column graphs comparing LMP7 and PSMB10 expression in tumor and TILs across ER+, HER2+ and TNBC subtypes. ***A.*** *mean %LMP7 in tumor,* ***B.*** *mean %PSMB10 expression in tumor,* ***C.*** *mean %LMP7 in TILs,* ***D.*** *mean %PSMB10 expression in TILs,* ***E.*** *mean LMP7 composite score in tumor,* ***F.*** *mean PSMB10 composite score in tumor,* ***G.*** *mean LMP7 composite score in TILs,* ***H.*** *mean PSMB10 composite score in TILs.*

3.6. ROC analyses

The LMP7 and PSMB10 expression had to be characterized into high and low. For this, ROC curves were plotted, and a value was selected which would give the maximum sensitivity and minimum 1-specificity. *(Fig 22 A-D)* shows the ROC curves for composite scores for LMP7 and PSMB10 in tumor and TILs. The final cut-offs are mentioned. If the cut-off was 3, all values ≤ 3 were taken as low expression, and all values >3 were taken as high expression.

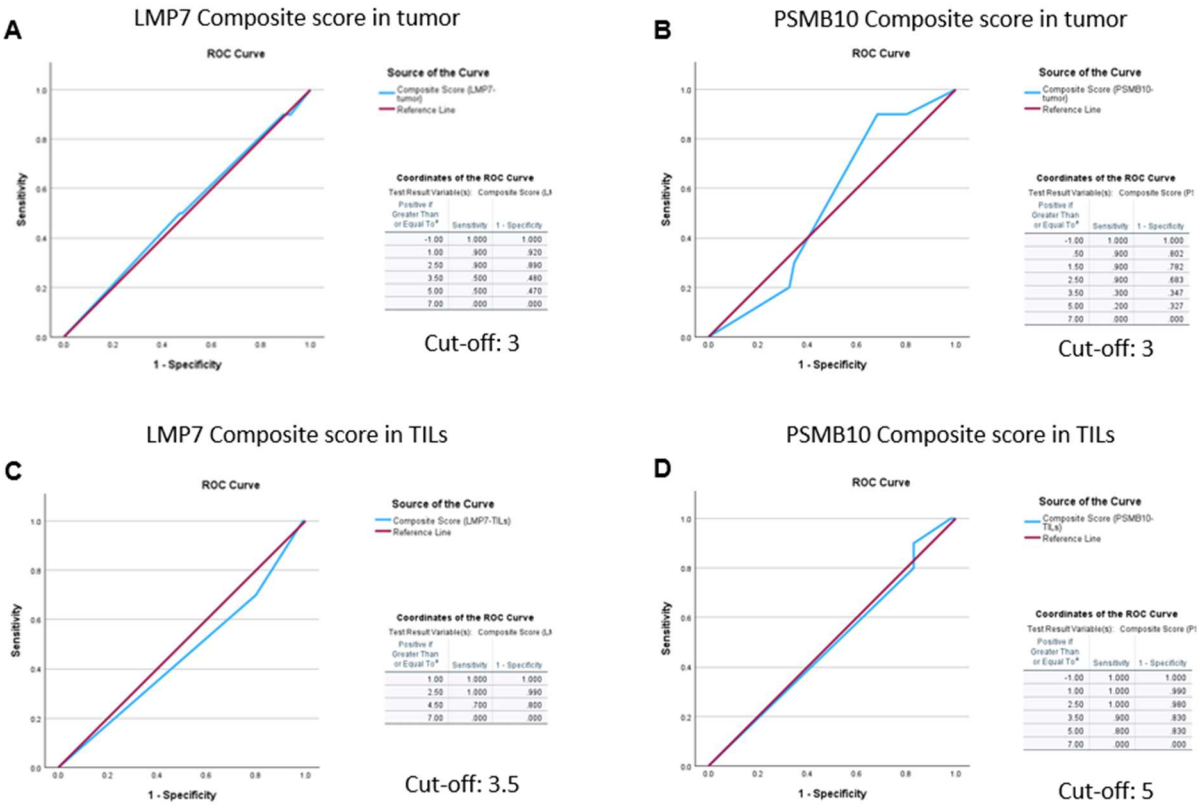

*Figure 22 : ROC curves for composite scores for composite scores of **A.** LMP7 in tumor, **B.** PSMB10 in tumor, **C.** LMP7 in TILs, **D.** PSMB10 in TILs. Curves plotted using IBM SPSS version 30 software.*

3.7. IP subunit expression and response to NACT

Out of 31 patients who received Neoadjuvant Chemotherapy (NACT), a higher percentage of patients with RD (residual disease) had a high composite score for LMP7 in tumor (74.19%) than low composite score (6.45%). Similarly, for PSMB10 in tumor also a higher percentage of patients with RD had a high composite score (48.39%) than low composite score (32.26%). But LMP7 in tumor had a higher RD as compared to PSMB10 in tumor *(Fig. 23).*

For IP expression in TILs, more patients with RD had a higher composite score, with no difference between LMP7 and PSMB10 *(Fig. 23).*

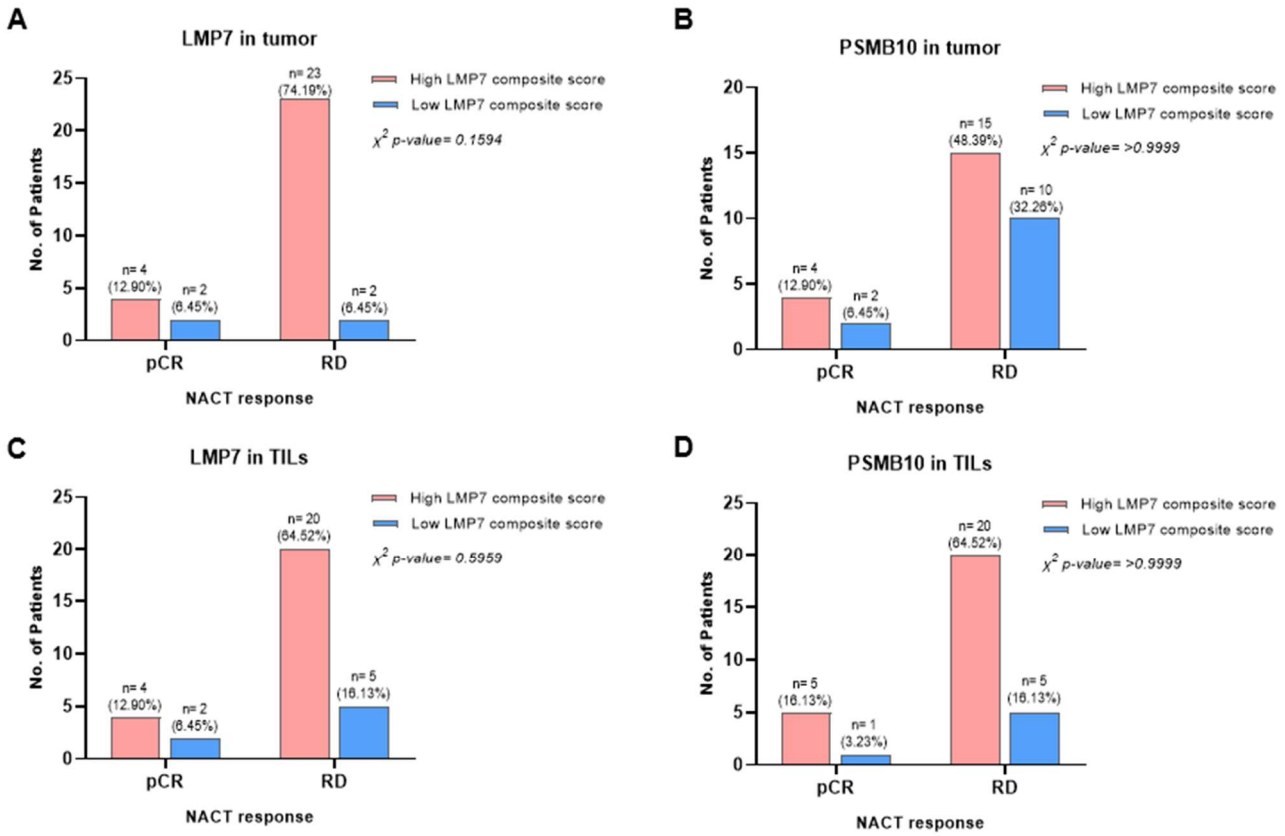

Figure 23: Bar plots for pCR and RD after NACT treatment for high vs low IP subunit expression of ***A.*** *LMP7 in tumor,* ***B.*** *PSMB10 in tumor,* ***C.*** *LMP7 in TILs,* ***D.*** *PSMB10 in TILs,*

3.8. IP subunit expression and patient survival outcomes

To study the association between the expression of the IP subunits LMP7 and PSMB10 with the patient outcomes, Kaplan-Meier survival plots for overall survival (OS) and Disease-free survival (DFS) were looked at.

OS is the time between the date of diagnosis and the death of the patient or the last follow-up date. DFS is the length of time between the date of first treatment and the date of recurrence of the disease. The OS and DFS plots show us how the patients

do in the long run with respect to the parameters that we want to study (example, a biomarker).

The OS and DFS graphs for LMP7 and PSMB10 in tumor are given in *(Fig 24).* Patients with high composite score for LMP7 and PSMB10 in tumor had a lower DFS than those with low composite score *(Fig. 24A, C).* A similar pattern was observed for their OS, but the separation was not big due to a smaller sample set and a smaller number of events of death *(Fig. 24B, D).*

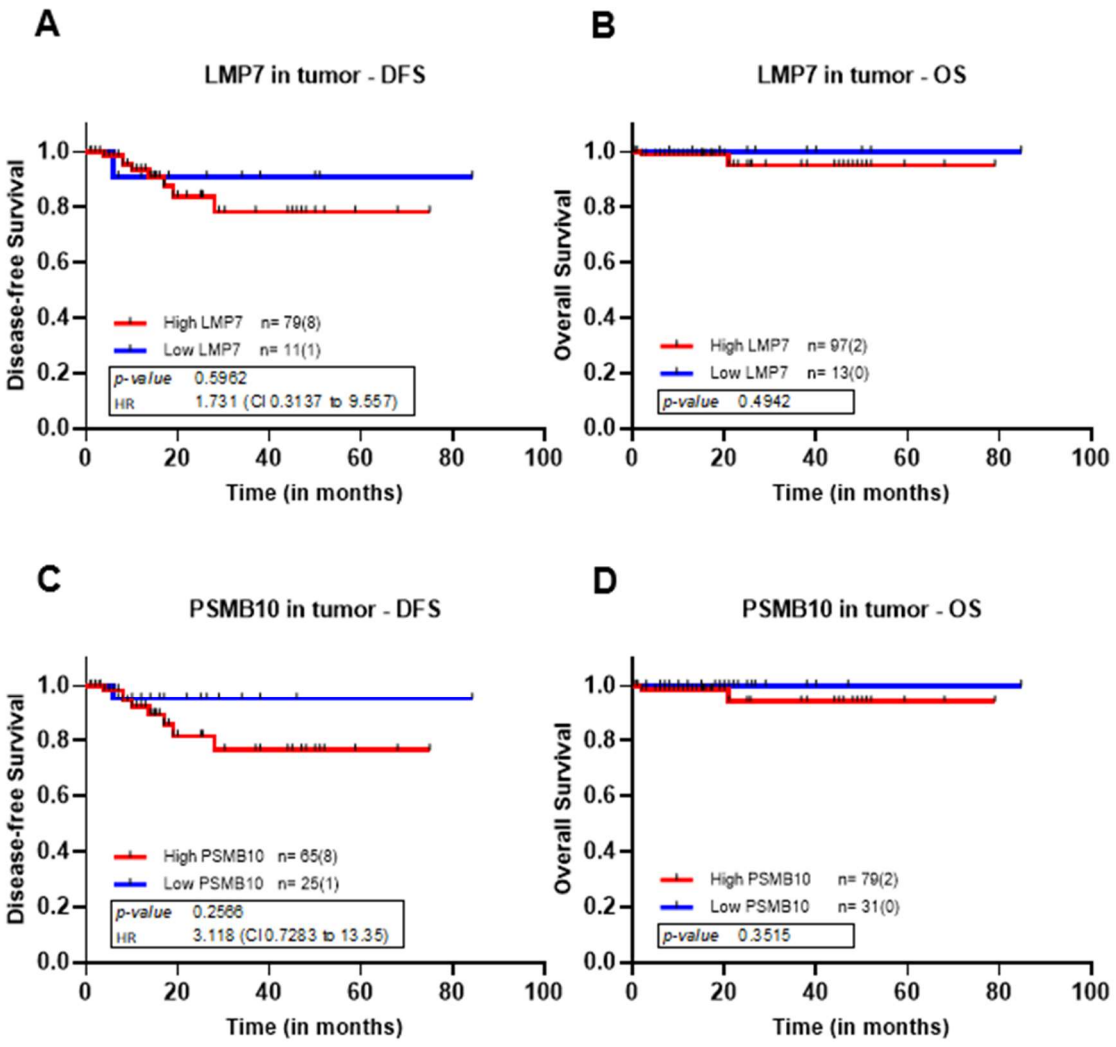

*Figure 24: Kaplan-Meier DFS plots for composite scores for **A.** LMP7 in tumor, **C.** PSMB10 in tumor, and OS plots for **B.** LMP7 in tumor, **d.** PSMB10 in tumor. **(**Data n.s.) Plotted using the IBM SPSS version 30 software*

For LMP7 and PSMB10 in TILs, the OS and DFS graphs are given in *(Fig 25).* No clear separation was seen for OS or DFS for high and low LMP7 and PSMB10 in TILs *(Fig. 25A, B, C, D).* A high LMP7 score in TILs showed higher DFS, but low OS. For PSMB10 in TILs, both OS and DFS were low for a higher expression (data insignificant).

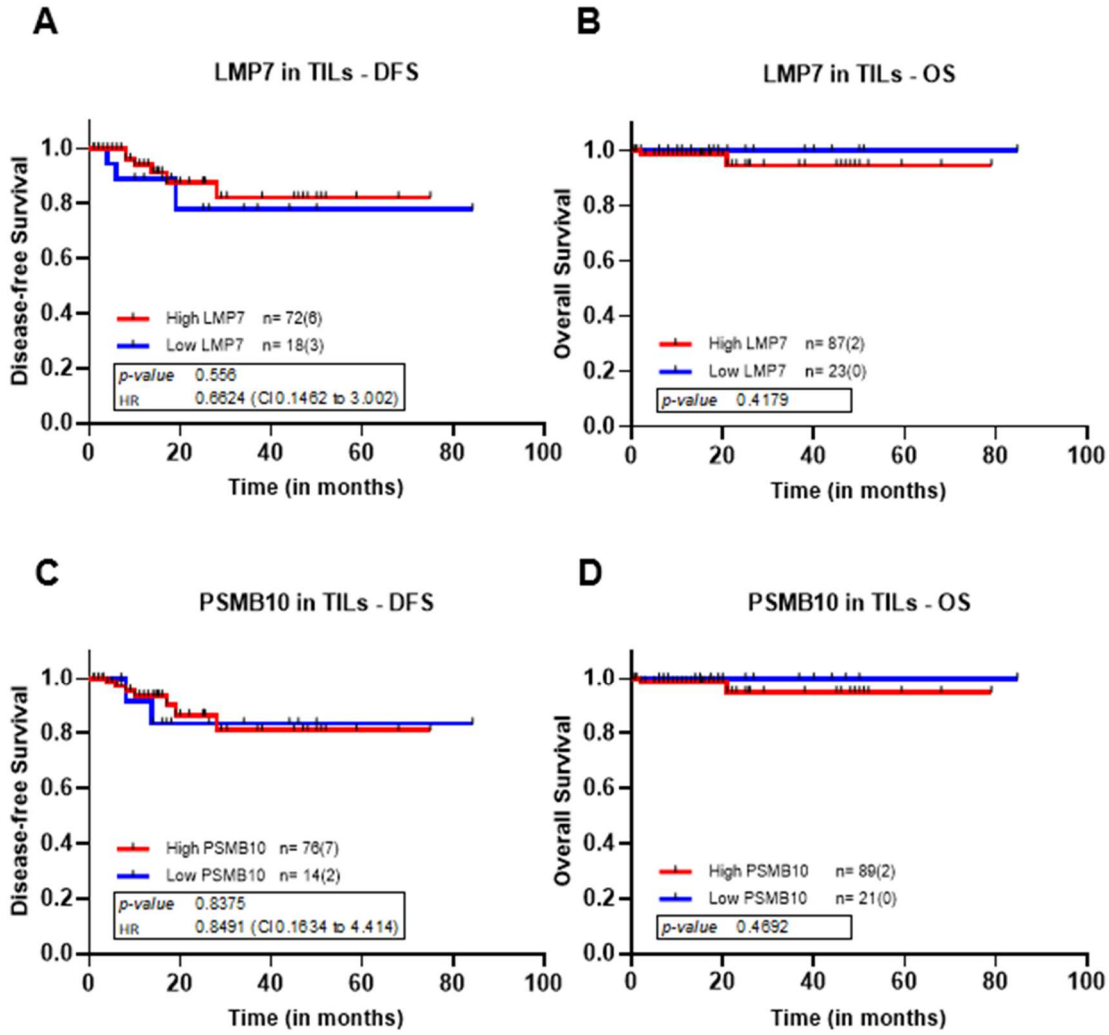

Figure 25: Kaplan-Meier DFS plots for composite scores for ***A.*** *LMP7 in TILs,* ***C.*** *PSMB10 in TILs, and OS plots for* ***B.*** *LMP7 in TILs,* ***D.*** *PSMB10 in TILs.* ***(****Data n.s.) Plotted using the IBM SPSS version 30 software*

3.9. IP subunit expression and subtype-wise patient survival outcomes

Upon looking at patient survival across molecular subtypes, it was observed that for all breast cancer molecular subtypes, patients with high composite score for LMP7 and PSMB10 in tumor had worse prognosis (OS ad DFS) *(Fig. 26).* High LMP7 in tumor had the lowest DFS for ER+ breast cancer, followed by TNBC and HER2+ breast cancers. Similar results (insignificant) were observed for PSMB10 in tumor. The subtype-wise OS had no separation for LMP7 or PSMB10.

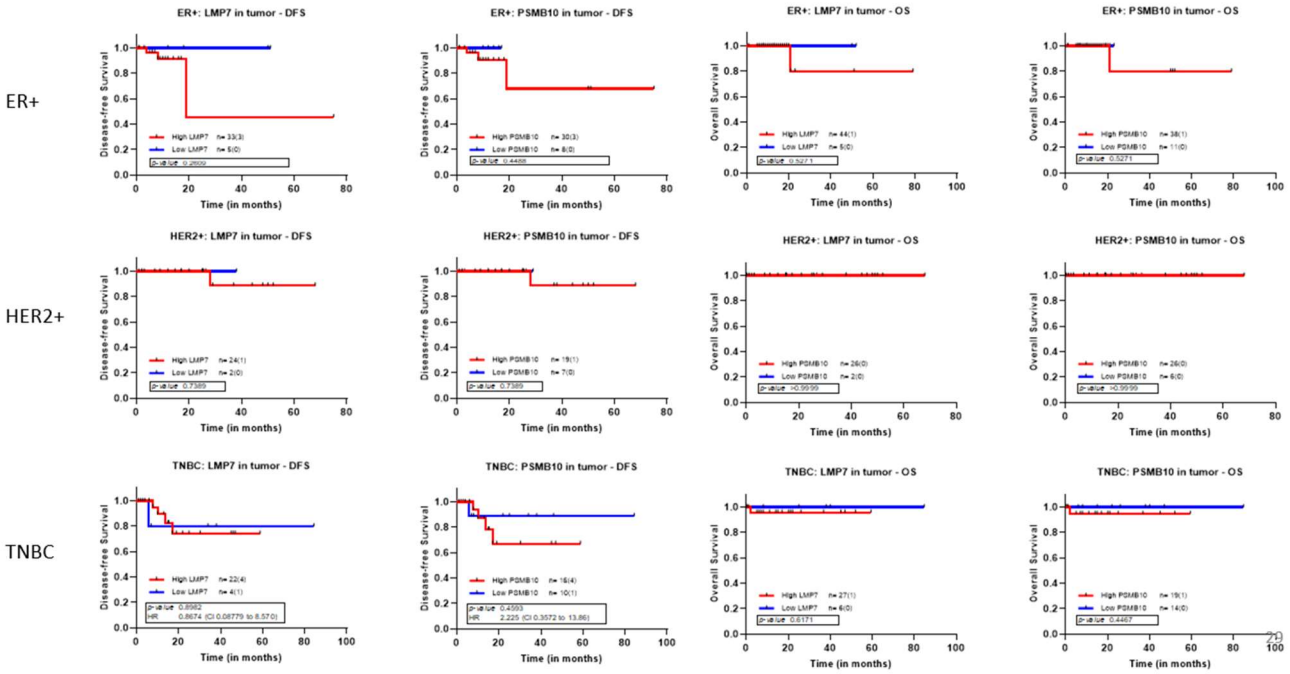

Figure 26: Kaplan-Meier for (left to right) DFS for LMP7 in tumor, PSMB10 in tumor, and OS for LMP7 in tumor, PSMB10 in tumor, across (top to bottom) molecular subtypes of breast cancer ER+, HER2+, TNBC. (Data n.s.) Plotted using the IBM SPSS version 30 software

For LMP7 and PSMB10 in TILs, again, there was no clear separation of OS and DFS for high and low IP expression *(Fig. 27).*

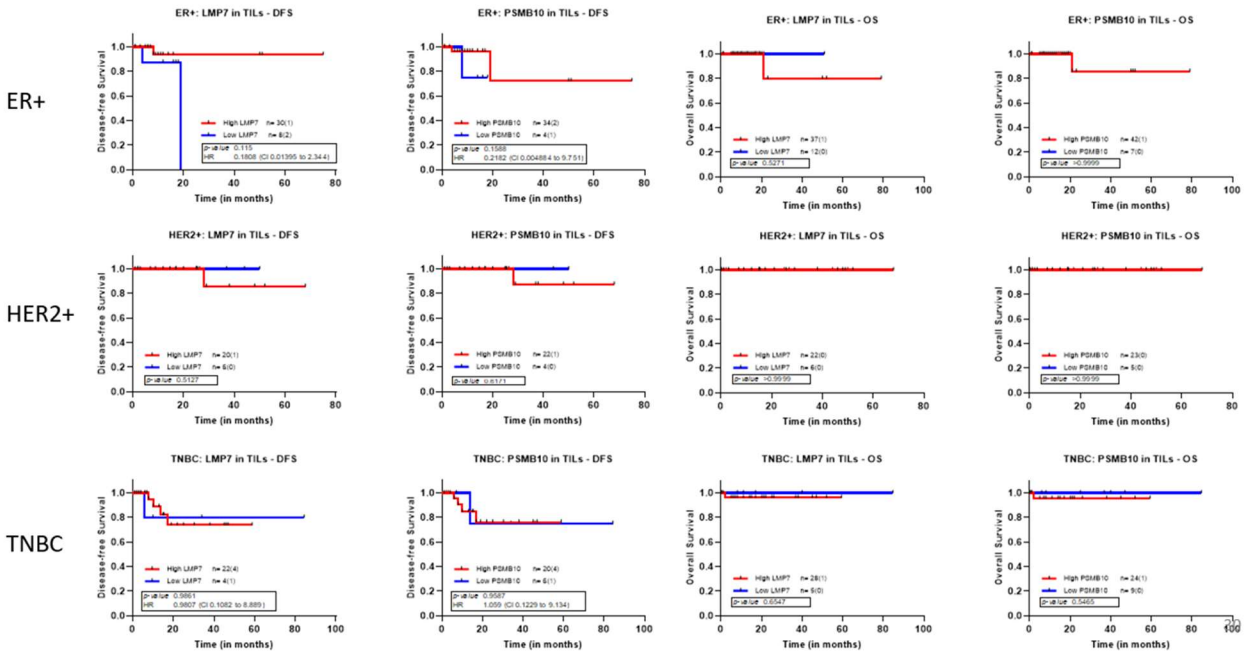

Figure 27: Kaplan-Meier for (left to right) DFS for LMP7 in TILs, PSMB10 in TILs, and OS for LMP7 in TILs, PSMB10 in TILs, across (top to bottom) molecular subtypes of breast cancer ER+, HER2+, TNBC. (Data n.s.) Plotted using the IBM SPSS version 30 software

Overall, no differences in the OS or DFS arise for LMP7 and PSMB10 in tumor or TILs because of the reduced number of samples in each molecular subtype.

4. Conclusion

This study highlights the complex role of immunoproteasomes in breast cancer, with differential expression in tumors and TILs correlating with immune infiltration and patient prognosis. Our findings suggest that:

- High IP expression in tumors correlates with lower TILs infiltration and worse survival
- TILs infiltration is independent of IP expression in the immune cells (here, TILs)
- IP expression in tumor is variable across breast cancer subtypes:

  LMP7 : HER2+ > ER+ > TNBC

  PSMB10: ER+ > HER2+ > TNBC

5. Discussion

Breast cancer is a disease with significant molecular and clinical variability. In the tumor microenvironment, a large number of molecules and pathways interact with each other and lead to initiation, progression and metastasis of the cancer. This study aimed to analyze the expression of immunoproteasome (IP) catalytic subunits LMP7 and PSMB10 in IDC breast cancer samples of an Indian cohort, correlating their expression with immune infiltration and the patient outcomes.

In this study on 135 breast cancer samples of ER+, HER2+, and TNBC subtypes, we found that there was a significant positive correlation between the expression of LMP7 and PSMB10 in tumor (r=0.3625, p<0.0001). This result was also seen in a study by (Lee et al., 2019b) where data from TCGA showed a high correlation between LMP7 and PSMB10 (r=.822, p=<*0.001*), further supporting our observations.

In contrast, no correlation was found between expression of LMP7 and PSMB10 in TILs (r=0.1182, p=0.1737). However, the comparison of LMP7 and PSMB10 expression between tumor and TILs showed a significant positive correlation (*p<0.0001),* which hints at the possibility of a feed-forward regulatory mechanism, where the IP expression in tumor or TILs may induce IP expression in the other. A similar mechanism has been explained by (Leister et al., 2021)

An interesting find was that the IP subunit expression in tumor was negatively correlated with the TILs infiltration (given by %TILs score). This finding suggests that the IP subunit upregulation in the tumor might contribute to an immunosuppressive environment and interfere with TILs recruitment.

When these correlations were analyzed within the breast cancer subtypes, we observed that while the statistical significance was lost in some cases, the direction of the correlation remained largely consistent across the different subtypes. With an increased number of samples, it can be investigated whether the immunoproteasome upregulation follows a conserved pattern across the breast cancer subtypes.

The expression levels of LMP7 were consistently higher than that of PSMB10 in both tumor and TILs, especially in tumor cells. The less stratification of LMP7 and PSMB10

expression in TILs could be because immune cells are known to predominantly express immunoproteasomes, and that their expression by non-immune cells is induced (by factors like INF-γ and TNF-α).

Next, to assess the clinical association of LMP7 and PSMB10 expression, we looked at patient response to neoadjuvant chemotherapy (NACT) as residual disease (RD) and pathological complete response (pCR) with respect to high or low IP expression. We found that a higher number of patients with RD had high LMP7 and PSMB10 expression in both tumor and TILs. But when the two subunits were compared, high LMP7 in tumor had higher RD as compared to PSMB10 in tumor, suggesting difference in the activity or role of the IP subunits in the breast tumor microenvironment.

We also analyzed disease-free survival (DFS) and overall survival (OS) curves for the patient data. We found that high LMP7 and PSMB10 expression in tumor cells was associated with worse DFS and OS. Though the data is not significant, it could suggest that the upregulation of immunoproteasome may lead to poor prognosis.

High vs low LMP7 and PSMB10 expression in TILs did not show a good separation. In the subtype-wise patient outcome analysis too we found that patients with high LMP7 and PSMB10 expression in tumor did worse than low expression in ER+, HER2+ and TNBC patients.

Interestingly, (Vaid et al., 2022) in her study showed that in breast cancer patients of an Indian cohort, patients with TNBC had higher TILs infiltration than patients with HER2+ or ER+ breast cancers. The study also showed that a higher proportion of breast cancer patients with high TILs had better pCR rates than patients with low TILs.

Our study shows that TNBC had the lowest IP expression, high IP expression was associated with lesser TILs and a worse prognosis.

Together, these studies validate each other’s findings as shown in *(Fig. 28).*

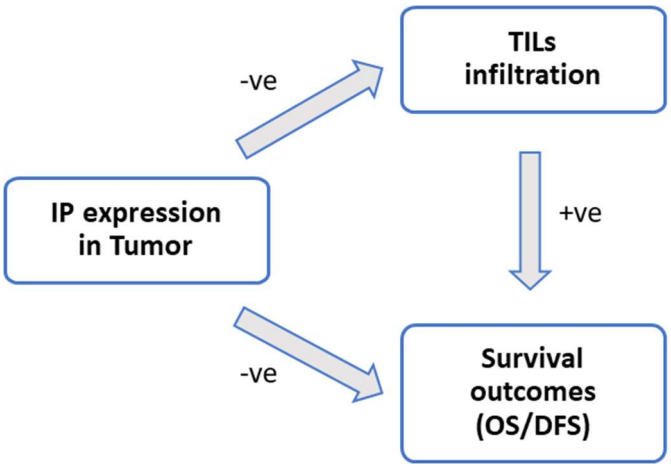

Figure 28: Schematic showing relation between IP, TILs, and patient prognosis

Immunoproteasomes are known to enhance antigen presentation and promote immune surveillance. However, our study shows a negative correlation between IP expression and TILs, making it counterintuitive and suggestive of a potential immunosuppressive role within the tumor microenvironment.

Moreover, TILs can comprise T-cells and B-cells, and within T-cells they could be CTLs, Tregs, or Th cells. It would be interesting to know which of these TILs express IP more prominently and which are most influenced by the IP expressed in tumor cells. Methods like H&E and IHC cannot distinguish between the types of TILs phenotypically. A future direction to the project could be to look into TILs as T-cell and B-cell populations using multiplex-immunofluorescence.

Additionally, investigating whether spatial proximity between tumor cells and TILs influences IP expression in TILs (or tumor) could provide further insights into the tumor-immune interactions in the TME with respect to IP.

Finally, a major limitation of the study is the limited sample size of the cohort. A larger sample size would lead to better statistical power, more significant subtype-wise analyses, and conclusive findings.

6. References

Abi Habib, J., Lesenfants, J., Vigneron, N., & Van den Eynde, B. J. (2022). Functional Differences between Proteasome Subtypes. *Cells*, *11*(3), 421. https://doi.org/10.3390/cells11030421

Aki, M., Shimbara, N., Takashina, M., Akiyama, K., Kagawa, S., Tamura, T., Tanahashi, N., Yoshimura, T., Tanaka, K., & Ichihara, A. (1994). Interferon-γ Induces Different Subunit Organizations and Functional Diversity of Proteasomes1. *The Journal of Biochemistry*, *115*(2), 257–269. https://doi.org/10.1093/oxfordjournals.jbchem.a124327

Balkwill, F. R., Capasso, M., & Hagemann, T. (2012). The tumor microenvironment at a glance. *Journal of Cell Science*, *125*(23), 5591–5596. https://doi.org/10.1242/jcs.116392

BARROSO-SOUSA, R., Sousa, I. M. de, Marin Comini, A. C., Celeste Tavares, M., Madasi Pinheiro, F., Bines, J., Dal Ponte Ferreira, R., Rosa, D. D., Santos, C. L., Souza, Z. S., Suzuki, D. A., de Araujo, J. A. P., Gagliato, D. D. M., Dos Anjos, C. H., Zucchetti, B. M., Ferrari, A. C. R. de C., Lopes De Brito, M., Monteiro, M. M. F., Testa, L., & Bonadio, R. C. (2024). Prediction of pathologic complete response to chemoimmunotherapy in triple-negative breast cancer using tumor-infiltrating lymphocytes: Exploiting cutoff values. *Journal of Clinical Oncology*, *42*(16_suppl), e12629–e12629. https://doi.org/10.1200/JCO.2024.42.16_suppl.e12629

de Visser, K. E., & Joyce, J. A. (2023). The evolving tumor microenvironment: From cancer initiation to metastatic outgrowth. *Cancer Cell*, *41*(3), 374–403. https://doi.org/10.1016/j.ccell.2023.02.016

Denkert, C., von Minckwitz, G., Darb-Esfahani, S., Lederer, B., Heppner, B. I., Weber, K. E., Budczies, J., Huober, J., Klauschen, F., Furlanetto, J., Schmitt, W. D., Blohmer, J. U., Karn, T., Pfitzner, B. M., Kümmel, S., Engels, K., Schneeweiss, A., Hartmann, A., Noske, A., … Loibl, S. (2018). Tumour-infiltrating lymphocytes and prognosis in different subtypes of breast cancer: a pooled analysis of 3771 patients treated with neoadjuvant therapy. *The Lancet Oncology*, *19*(1), 40–50. https://doi.org/10.1016/S1470-2045(17)30904-X

Driscoll, J., Brown, M. G., Finley, D., & Monaco, J. J. (1993). MHC-linked LMP gene products specifically alter peptidase activities of the proteasome. *Nature*, *365*(6443), 262–264. https://doi.org/10.1038/365262a0

Du, S. H., Xiang, Y. J., Liu, L., Nie, M., Hou, Y., Wang, L., Li, B. B., Xu, M., Teng, Q. L., Peng, J., Hou, M., & Shi, Y. (2021). Co-Inhibition of the Immunoproteasome Subunits LMP2 and LMP7 Ameliorates Immune Thrombocytopenia. *Frontiers in Immunology*, *11*. https://doi.org/10.3389/fimmu.2020.603278

Fanale, D., Dimino, A., Pedone, E., Brando, C., Corsini, L. R., Filorizzo, C., Fiorino, A., Lisanti, M. C., Magrin, L., Randazzo, U., Bazan Russo, T. D., Russo, A., & Bazan, V. (2022). Prognostic and Predictive Role of Tumor-Infiltrating Lymphocytes (TILs) in Ovarian Cancer. *Cancers*, *14*(18), 4344. https://doi.org/10.3390/cancers14184344

Frankowska, K., Zarobkiewicz, M., Dąbrowska, I., & Bojarska-Junak, A. (2023). Tumor infiltrating lymphocytes and radiological picture of the tumor. *Medical Oncology (Northwood, London, England)*, *40*(6), 176. https://doi.org/10.1007/s12032-023-02036-3

Gao, G., Wang, Z., Qu, X., & Zhang, Z. (2020). Prognostic value of tumor-infiltrating lymphocytes in patients with triple-negative breast cancer: a systematic review and meta-analysis. *BMC Cancer*, *20*(1), 179. https://doi.org/10.1186/s12885-020-6668-z

Hong, J., Rui, W., Fei, X., Chen, X., & Shen, K. (2021). Association of tumor-infiltrating lymphocytes before and after neoadjuvant chemotherapy with pathological complete response and prognosis in patients with breast cancer. *Cancer Medicine*, *10*(22), 7921–7933. https://doi.org/10.1002/cam4.4302

Howlader, N., Cronin, K. A., Kurian, A. W., & Andridge, R. (2018). Differences in Breast Cancer Survival by Molecular Subtypes in the United States. *Cancer Epidemiology, Biomarkers & Prevention*, *27*(6), 619–626. https://doi.org/10.1158/1055-9965.EPI-17-0627

Kalaora, S., Lee, J. S., Barnea, E., Levy, R., Greenberg, P., Alon, M., Yagel, G., Bar Eli, G., Oren, R., Peri, A., Patkar, S., Bitton, L., Rosenberg, S. A., Lotem, M., Levin, Y., Admon, A., Ruppin, E., & Samuels, Y. (2020). Immunoproteasome expression is associated with better prognosis and response to checkpoint therapies in melanoma. *Nature Communications*, *11*(1), 896. https://doi.org/10.1038/s41467-020-14639-9

Kirkby, M., Popatia, A. M., Lavoie, J. R., & Wang, L. (2023). The Potential of Hormonal Therapies for Treatment of Triple-Negative Breast Cancer. *Cancers*, *15*(19), 4702. https://doi.org/10.3390/cancers15194702

Kotamraju, S., Matalon, S., Matsunaga, T., Shang, T., Hickman-Davis, J. M., & Kalyanaraman, B. (2006). Upregulation of immunoproteasomes by nitric oxide: Potential antioxidative mechanism in endothelial cells. *Free Radical Biology and Medicine*, *40*(6), 1034–1044. https://doi.org/10.1016/j.freeradbiomed.2005.10.052

Kotamraju, S., Tampo, Y., Keszler, A., Chitambar, C. R., Joseph, J., Haas, A. L., & Kalyanaraman, B. (2003). Nitric oxide inhibits H_2O_2-induced transferrin receptor-dependent apoptosis in endothelial cells: Role of ubiquitin-proteasome pathway. *Proceedings of the National Academy of Sciences*, *100*(19), 10653–10658. https://doi.org/10.1073/pnas.1933581100

Kulkarni, A., Kelkar, D. A., Parikh, N., Shashidhara, L. S., Koppiker, C. B., & Kulkarni, M. (2020). Meta-Analysis of Prevalence of Triple-Negative Breast Cancer and Its Clinical Features at Incidence in Indian Patients With Breast Cancer. *JCO Global Oncology*, *6*, 1052–1062. https://doi.org/10.1200/GO.20.00054

Kumar, R., Dhaka, B., Sahoo, S., Jolly, M. K., & Sabarinathan, R. (2023). Prognostic association of immunoproteasome expression in solid tumours is governed by the immediate immune environment. *Molecular Oncology*, *17*(6), 1041–1059. https://doi.org/10.1002/1878-0261.13443

Lee, M., Song, I. H., Heo, S.-H., Kim, Y.-A., Park, I. A., Bang, W. S., Park, H. S., Gong, G., & Lee, H. J. (2019a). Expression of Immunoproteasome Subunit LMP7 in Breast Cancer and Its Association with Immune-Related Markers. *Cancer Research and Treatment*, *51*(1), 80–89. https://doi.org/10.4143/crt.2017.500

Lee, M., Song, I. H., Heo, S.-H., Kim, Y.-A., Park, I. A., Bang, W. S., Park, H. S., Gong, G., & Lee, H. J. (2019b). Expression of Immunoproteasome Subunit LMP7 in Breast Cancer and Its Association with Immune-Related Markers. *Cancer Research and Treatment*, *51*(1), 80–89. https://doi.org/10.4143/crt.2017.500

Leister, H., Krause, F. F., Mahdavi, R., Steinhoff, U., & Visekruna, A. (2022). The Role of Immunoproteasomes in Tumor-Immune Cell Interactions in Melanoma and Colon Cancer. In

Archivum Immunologiae et Therapiae Experimentalis (Vol. 70, Issue 1). Springer Science and Business Media Deutschland GmbH. https://doi.org/10.1007/s00005-022-00644-x

Leister, H., Luu, M., Staudenraus, D., Lopez Krol, A., Mollenkopf, H.-J., Sharma, A., Schmerer, N., Schulte, L. N., Bertrams, W., Schmeck, B., Bosmann, M., Steinhoff, U., & Visekruna, A. (2021). Pro- and Antitumorigenic Capacity of Immunoproteasomes in Shaping the Tumor Microenvironment. *Cancer Immunology Research*, *9*(6), 682–692. https://doi.org/10.1158/2326-6066.CIR-20-0492

Li, H., Courtois, E. T., Sengupta, D., Tan, Y., Chen, K. H., Goh, J. J. L., Kong, S. L., Chua, C., Hon, L. K., Tan, W. S., Wong, M., Choi, P. J., Wee, L. J. K., Hillmer, A. M., Tan, I. B., Robson, P., & Prabhakar, S. (2017). Reference component analysis of single-cell transcriptomes elucidates cellular heterogeneity in human colorectal tumors. *Nature Genetics*, *49*(5), 708–718. https://doi.org/10.1038/ng.3818

Liu, S., Lachapelle, J., Leung, S., Gao, D., Foulkes, W. D., & Nielsen, T. O. (2012). CD8+ lymphocyte infiltration is an independent favorable prognostic indicator in basal-like breast cancer. *Breast Cancer Research*, *14*(2), R48. https://doi.org/10.1186/bcr3148

Magnussen, A. L., & Mills, I. G. (2021). Vascular normalisation as the stepping stone into tumour microenvironment transformation. *British Journal of Cancer*, *125*(3), 324–336. https://doi.org/10.1038/s41416-021-01330-z

Masood, S. (2016). Breast Cancer Subtypes: Morphologic and Biologic Characterization. *Women's Health*, *12*(1), 103–119. https://doi.org/10.2217/whe.15.99

Milosevic, V., & Östman, A. (2024). Interactions between cancer-associated fibroblasts and T-cells: functional crosstalk with targeting and biomarker potential. *Upsala Journal of Medical Sciences*, *129*, e10710. https://doi.org/10.48101/ujms.v129.10710

Monaco, J. J., & McDevitt, H. O. (1986). The LMP antigens: A stable MHC-controlled multisubunit protein complex. *Human Immunology*, *15*(4), 416–426. https://doi.org/10.1016/0198-8859(86)90019-4

Plasilova, M. L., Hayse, B., Killelea, B. K., Horowitz, N. R., Chagpar, A. B., & Lannin, D. R. (2016). Features of triple-negative breast cancer. *Medicine*, *95*(35), e4614. https://doi.org/10.1097/MD.0000000000004614

Quail, D. F., & Joyce, J. A. (2013). Microenvironmental regulation of tumor progression and metastasis. *Nature Medicine*, *19*(11), 1423–1437. https://doi.org/10.1038/nm.3394

Rana, P. S., Ignatz-Hoover, J. J., Guo, C., Mosley, A. L., Malek, E., Federov, Y., Adams, D. J., & Driscoll, J. J. (2024). Immunoproteasome Activation Expands the MHC Class I Immunopeptidome, Unmasks Neoantigens, and Enhances T-cell Anti-Myeloma Activity. *Molecular Cancer Therapeutics*, *23*(12), 1743–1760. https://doi.org/10.1158/1535-7163.MCT-23-0931

Salgado, R., Denkert, C., Demaria, S., Sirtaine, N., Klauschen, F., Pruneri, G., Wienert, S., Van den Eynden, G., Baehner, F. L., Penault-Llorca, F., Perez, E. A., Thompson, E. A., Symmans, W. F., Richardson, A. L., Brock, J., Criscitiello, C., Bailey, H., Ignatiadis, M., Floris, G., … Loi, S. (2015). The evaluation of tumor-infiltrating lymphocytes (TILs) in breast cancer: recommendations by an International TILs Working Group 2014. *Annals of Oncology*, *26*(2), 259–271. https://doi.org/10.1093/annonc/mdu450

Tripathi, S. C., Peters, H. L., Taguchi, A., Katayama, H., Wang, H., Momin, A., Jolly, M. K., Celiktas, M., Rodriguez-Canales, J., Liu, H., Behrens, C., Wistuba, I. I., Ben-Jacob, E., Levine, H., Molldrem, J. J., Hanash, S. M., & Ostrin, E. J. (2016). Immunoproteasome deficiency is a feature of non-small cell lung

cancer with a mesenchymal phenotype and is associated with a poor outcome. *Proceedings of the National Academy of Sciences*, *113*(11). https://doi.org/10.1073/pnas.1521812113

Ungefroren, H., Sebens, S., Seidl, D., Lehnert, H., & Hass, R. (2011). Interaction of tumor cells with the microenvironment. *Cell Communication and Signaling*, *9*(1), 18. https://doi.org/10.1186/1478-811X-9-18

Vaid, P. M., Puntambekar, A. K., Jumle, N. S., Banale, R. A., Ansari, D., Reddy, R. R., Unde, R. R., Namewar, N. P., Kelkar, D. A., Shashidhara, L. S., Koppiker, C. B., & Kulkarni, M. D. (2022). Evaluation of tumor-infiltrating lymphocytes (TILs) in molecular subtypes of an Indian cohort of breast cancer patients. *Diagnostic Pathology*, *17*(1). https://doi.org/10.1186/s13000-022-01271-y

Vigneron, N., & Van den Eynde, B. (2014). Proteasome Subtypes and Regulators in the Processing of Antigenic Peptides Presented by Class I Molecules of the Major Histocompatibility Complex. *Biomolecules*, *4*(4), 994–1025. https://doi.org/10.3390/biom4040994

Wang, J., He, Y., Hu, F., Hu, C., Sun, Y., Yang, K., & Yang, S. (2024). Metabolic Reprogramming of Immune Cells in the Tumor Microenvironment. *International Journal of Molecular Sciences*, *25*(22), 12223. https://doi.org/10.3390/ijms252212223

Yang, W., Liu, S., Mao, M., Gong, Y., Li, X., Lei, T., Liu, C., Wu, S., & Hu, Q. (2024a). T-cell infiltration and its regulatory mechanisms in cancers: insights at single-cell resolution. *Journal of Experimental & Clinical Cancer Research*, *43*(1), 38. https://doi.org/10.1186/s13046-024-02960-w

Yang, W., Liu, S., Mao, M., Gong, Y., Li, X., Lei, T., Liu, C., Wu, S., & Hu, Q. (2024b). T-cell infiltration and its regulatory mechanisms in cancers: insights at single-cell resolution. *Journal of Experimental & Clinical Cancer Research*, *43*(1), 38. https://doi.org/10.1186/s13046-024-02960-w

Yuan, Z., Li, Y., Zhang, S., Wang, X., Dou, H., Yu, X., Zhang, Z., Yang, S., & Xiao, M. (2023). Extracellular matrix remodeling in tumor progression and immune escape: from mechanisms to treatments. *Molecular Cancer*, *22*(1), 48. https://doi.org/10.1186/s12943-023-01744-8

Zhu, C., Zhao, Y., He, J., Zhao, H., Ni, L., Cheng, X., Chen, Y., Mu, L., Zhou, X., Shi, Q., & Sun, J. (2023). TIL-Derived CAR T Cells Improve Immune Cell Infiltration and Survival in the Treatment of CD19-Humanized Mouse Colorectal Cancer. *Cancers*, *15*(23), 5567. https://doi.org/10.3390/cancers15235567